OPTIMIZED DEGENERATE CHEMICAL DOPING TOWARD P-WSe_2 FET

Yasir Hassan

Reg. No. NUST201362361MSCME67913F

(MS in Nano Science & Engineering)

Supervisor:
Dr. Iftikhar Hussain Gul

School of Chemical & Materials Engineering (SCME)

National University of Science and Technology

Islamabad, Pakistan

February, 2016

CERTIFICATE

*This is to certify that the work in this dissertation has been carried out by **Mr. Yasir Hassan** and completed under my supervision at school of Chemical and Material Engineering, National University of Science and Technology, Islamabad, Pakistan.*

*Supervisor:*_____
Dr.Iftikhar Hussain Gul

*Co-Supervisor:*_____
Prof. Won Jong Yoo

Submitted through:

_____
Dr. Muhammad Shahid
Head of Department (ME)

Dedicated to

My Parents Brothers and Sister.

Abstract

Here in this work we have presented a chemical way of doping few layers (thickness ~12nm) WSe_2 to get a high performance p-type field effect transistor (FET). For this, $AuCl_3$ mix with acetonitrile is used as a chemical dopant for WSe_2 FET. Upon the reaction of $AuCl_3$ with WSe_2 the Au^{+3} reduces to stable Au^0 particle leaving behind a p-WSe_2 FET.

The effect of chemical doping on WSe_2 with $AuCl_3$ as a dopant is confirmed by changing of Pd and WSe_2 barrier from Schottkey to Ohmic-like behavior. In this case the doping helps in reduction of contact resistance by thinning the width of the barrier which helps in tunneling the hole from Pd contact to WSe_2 as a result the hole mobility of our device is increases from 0.26 cm^2/V.S to 149 cm^2/V.S at 10 mM concentration of $AuCl_3$ which is the highest achievement ever by doping in TMDC materials.

Here we have also investigated a stable and optimized value of doping concentration to get highly p-doped WSe_2 device. From the results we have concluded that at 10 mM concentration of $AuCl_3$ we can get a 10^4 time enhancement in ON current a 1000 times increase in conductivity and a shift of 75V in the threshold voltage after doping. Chemical doping of WSe_2 with $AuCl_3$ chemical dopant is highly stable and efficient way for achieving highly doped P-WSe_2 FET, and this study will prove promising to realize highly efficient complementary device.

Acknowledgment

With the blessing of all almighty Allah, the most charitable, forgiving and the creator of this beautiful world, today i am able to acknowledge after a fruitful completion of my research project. I also present my thanks in a modest and heartfelt way to the Prophet Muhammad (P.B.U.H) on behalf of which this universe exists. An inspirational messenger from Allah and great teacher who teach us the way of life and humanity.

I would like to thanks my supervisor Dr. Iftikhar Hussain Gul, who showed his kind interest in carrying this project, give me his precious time for complete guidance and fruitful advices during the whole research period. I feel proud to be his student. I will be thankful to him for my whole life.

I specially acknowledge my co-supervisor Prof. Won Jong Yoo from Sungkyunkwan University (SKKU), South Korea for assigning me to this project, give me this opportunity to work in his lab “Nano Device and Processing Lab (NDPL)” under his supervision and allow me to use lab stuffs and equipment for the completion of this project. His generous advices are one of the key factor results in successfully completing this research work. I will always remember his kind support and corporation in my life.

I present my gratitude to my entire lab mates, class fellows for being so kind, humble and keeping friendly environment with me during the whole period of my stay in the lab especially Mr. Faisal Ahmad for his back support and advices from start to end of this project and his help in learning all the related equipment in the lab. I think without his effort I will be unable to complete this work in time.

It will be a great pleasure for me to acknowledge my parents, brothers, sister and especially my sweet uncle Mr. Hamid-Ul-Haq who financially support me during the entire period of my study at SKKU.

Last but not the least I wish to thanks “National University of Science and Technology (NUST)” who give me this opportunity to study abroad and to the whole team of “NUST International Collaboration (NIC)” for processing my application form and collaborating with SKKU international office.

_____

Yasir Hassan

Contents

Pages

List of Figures

Figure 10: Lift off and annealing. **(a)** Substrate with deposited metal on the surface **(b)** Substrate in acetone for removal of excessive metal from the surface of the substrate **(d)** Drying of the sample using nitrogen gun **(d)** Sample on the RTA stage for annealing at 250 ^{0}C for 2 hrs.

Figure 11: Doping process through schlenk line setup, **(a)** Stirring of acetonitrile at 300rpm for 20 mints **(b)** Mixture of acetonitrile and gold chloride **(c)** Spin coating of dopant on the surface of wafer **(d)** Annealing after spin coating for 10mints at 100^{0}C.

Figure 12: Measurement of the device using four-probe station with device on the Cu substrate and probes are connected via Source (S), Drain (D) and Gate (G).

Figure 13: The Optical Microscope (OM) (a) Switch (b) CCD Camera (c) Computer- eye piece switch pin (d) Objectives (e) Sample stage (f, g) Horizontal and vertical caliber knob (h) Magnifying knob.

Figure 14: Vacuum Probe Station. (a, b, c, d) four probe aligners (e) Vacuum chamber (f, g) light source and magnifying glass (h) Vertical caliber knob (i) CCD camera (k) Laser source.

Figure 15: (A) Inside view of the vacuum chamber (l) source tip (m) gate tip (n) drain tip (B) Analyzer.

Figure 16: Electron beam lithography (EBL).

Figure 17: Schematic internal diagram of EBL.

Figure 18: Electron beam deposition (EBD).

Figure 19: Rapid Thermal Annealing (RTA). (a, b, c, d) Starting knobs (e) Computer (f) Output screen (g) Annealing chamber (h) Gas cylinder (i) Meter.

Figure 20: Glove Box (a) Small vacuum chamber (b) Pressure monitoring screen.

Figure 21: Schlenk line Process.

Figure 22: Atomic Force Microscopy (AFM) (a) Parameters controlling monitor (b) Output monitor connected with CCD camera.

Figure 23: 3D image of the back gated field effect transistor.

Figure 24: Electrical results of our device before and after doping. (a,b) shows the output curve at different V_g, before and after doping respectively. (c,d) denotes the transfer curve at different V_d before and after doping respectively.

Figure 25: The doping effect on device mobility. (a) Graph of the transconductance with respect to gate voltage before doping showing a decrease in slope as V_g moves toward negative value. (b) Shows the transconductance after doping with an increase in slop as the V_g value increase positively. (c) The calculated mobility with respect to doping concentration after doping showing a higher mobility at 10mM concentration.

Figure 26: Energy band diagram of metal-WSe2 device and doping effect. (a) The flat band structure of WSe_2 with Pd contact. (b) The band diagram of WSe_2 device after contact is made. (c) The band structure after doping with thinning the barrier width near the valance band and the tunneling of hole through the barrier.

Figure 27: Schematic diagram of doping mechanism with $AuCl_3$.

Introduction:

Most of the layered materials in 1970 and onward have been studied and used as an arid lubricant due to their atomically stable layered structure. Around 70 years ago, Physicist Lev Landa suggested that two dimensional materials are not thermodynamically stable structure.[24] But ever since the first exfoliation of single layer of graphite i.e. graphene, due to its Vander Waals layered structure, the researchers are excited towards 2D materials. Besides graphene a number of other 2D materials like Hexagonal Boron Nitride (hBN), Transition-metal Dichalcogenide (TMDCs), black Phosphorus (BP) and many others are also successfully extracted down to their monolayer form. All of them showed promising characteristics due to their auspicious electrical, optical and mechanical properties. [1-12] In comparison with their bulk counterpart materials like Si, the 2D materials show some exceptional properties like pristine surface, quantum confinement effect, ultrathin and flat body, mechanical flexibility and so on. Among 2D materials, graphene showed exceptional properties but lacks in band gap. The main parameter which shows superiority of TMDCs over graphene is their variable band gap i.e. Graphene has zero band gap and TMDCs have thickness dependent band gap i.e. it alters from indirect to direct band gap as the thickness goes from bulk to few and monolayers.[2] In perspective of photovoltaic application TMD's materials have the capability of absorbing much light and recognition of diverse wavelength just by only changing the thickness of the material (altering the numbers of layers).[13] In perspective of electronic properties, TMDC's material shields an extensive range of electromagnetic spectrum as shown in Fig 1.[25] From the family of layered material Molybdenum (Mo) and Tungsten (W) centered between Selenide (Se) or Sulfide (S) are semiconductors which are currently widely studied due to their stable crystal structure.[2] The physical structure of these material is such that, every "Mo" and "W" atoms are covalently bonded to two "Se" or "S" atoms that forms a stable sheets and these sheets are held together by weak Vander Waal force forming a readily peelable layered structure [Fig 2].

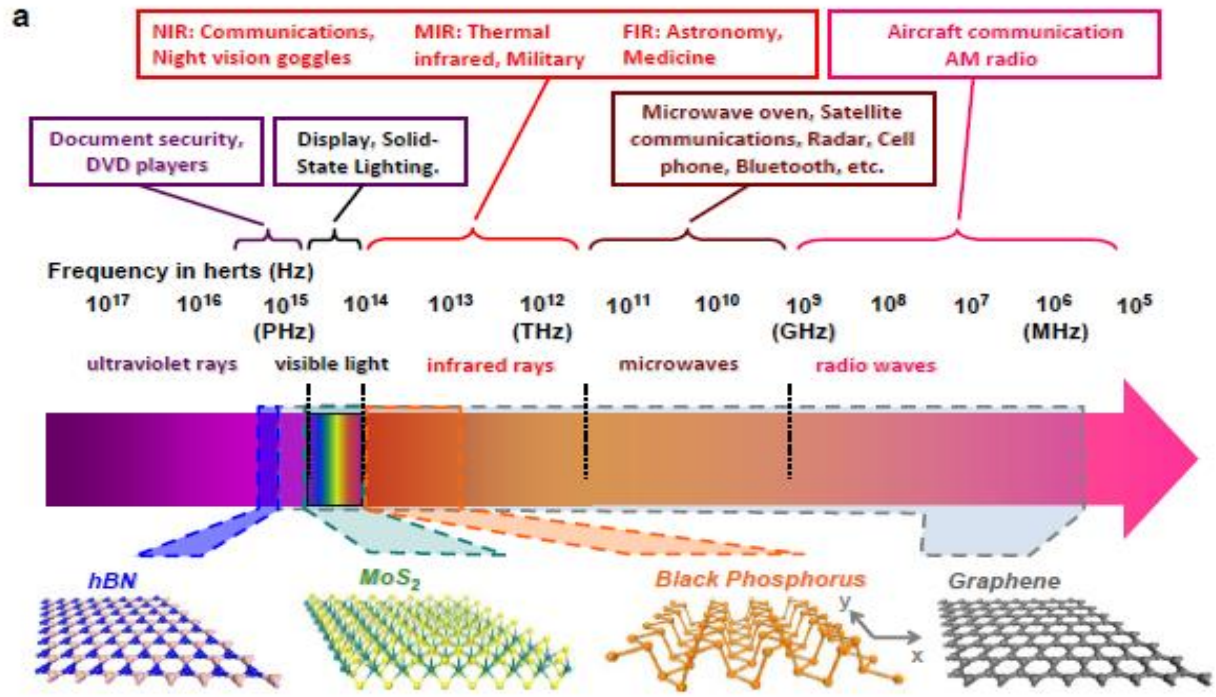

Figure 1: Two dimensional materials shielding a wide spectral range.[25]

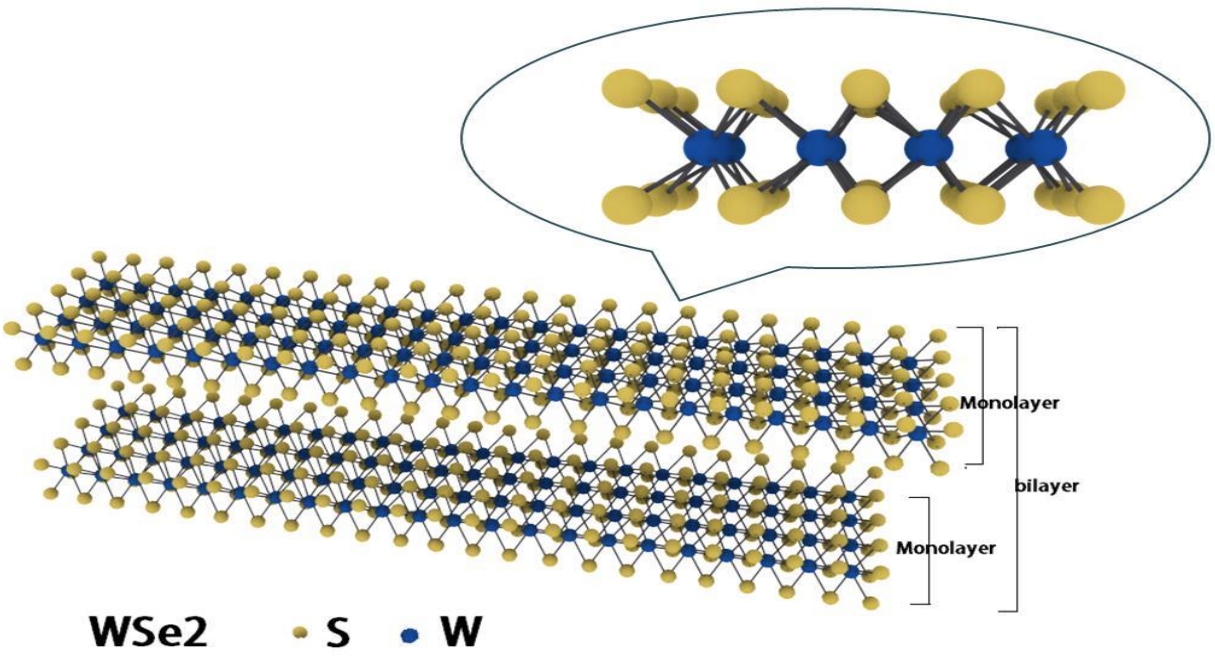

Figure 2: 3D image of the bilayer WSe_2.

MoS_2 in its bulk state maintain an indirect band gap of E_g=1.2eV but in its monolayer state it has a direct band gap of E_g=1.9eV similarly WSe_2 also has an indirect band gap of E_g=0.9~1.2eV in bulk state and a direct band gap of E_g~1.6eV [Fig.3].[3, 10, 14]

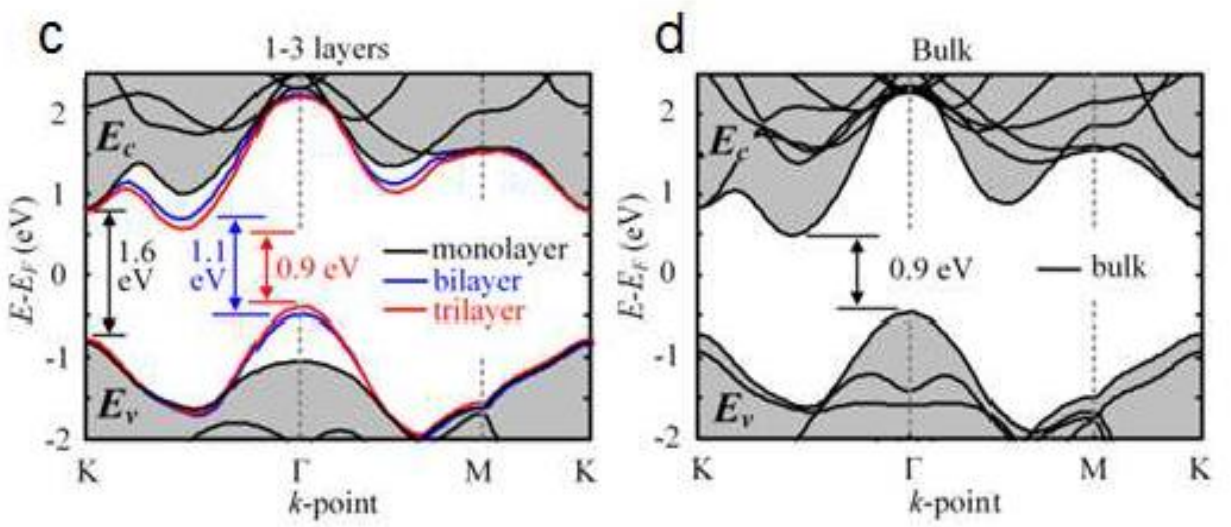

Figure 3: The band diagram of WSe2 with transition from indirect to direct w.r.t layers.[3]

Generally, for semiconductors the position of the Fermi energy level (E_f) shows the nature of the material i.e. p-type, n-type or ambipolar. For WSe_2, the Fermi level lies nearly adjacent to the intrinsic level (E_i) that enable it an ambipolar material unlike unipolar (n-type) MoS_2. That's why researchers are excited towards WSe_2 for electronic and optoelectronic applications.[4-11] To enhance the performance of device based on TMDs material different techniques are applied like selective metal for its source/drain contacts etc. The channel length dependency related to WSe_2 FET was studied by W.Liu and its co-workers presenting that monolayer WSe_2 is an appropriate material for ultra-short channel (sub 5-nm) FET with Silver "Ag" contacts.[3] *Allain and Kis.* studied the temperature dependency on WSe_2 FET and the related transport mechanism of electrons and holes from source to drain, further they claim that by using a polymer as a electrolyte gate helps us in converting a Shockley behavior into an Ohmic like behavior. [26] Tosun *et al.* used a high work function material (Pt/Au/Pd) to get high performance p-WSe_2 FET.[4] However; Liu *et al.* testified n-WSe_2 FET by using "Ag", a low work function material as a metal contact.[5] Besides from single use of theses material heterostructure made from TMDC's has one of the most attractive approach of the researchers. Different techniques have been applied by researchers to make heterostructure of MoS_2 and WSe_2 and with other TMDC's

material like Black Phosphorous (BP) and Indium Arsenide (InAs). To study the electroluminescence (EL) and photoluminescence (PL) of TMDC's material a heterostructure of WSe_2/MoS_2 was synthesized using Physical Vapor Deposition (PVD) on Si/SiO_2 substrate using alumina as forerunner by Rui. Cheng and its co-workers.[27] Similarly Jung Ho Yo synthesized the vertical heterostructure of WSe_2/MoS_2 followed by transferring into a substrate using polymer based transfer method which results in a vertical align layered of these materials.[28] A lateral heterojunction of WSe_2 with $MoSe_2$ was successfully achieved and presented by Chunming Huang et al in his article by vapour-solid growth and a simple PMMA transferring method.[29] In comparison WSe_2 was also fabricated with Indium Arsenide (InAs) to form a van der Waals heterojunction diodes by Ali Javey group to study its near-ideal electrical properties using a conventional epitaxial technique.[30] TMDC's can also be synthesize using a common chemical vapor deposition (CVD) technique. Hailong Zhou in its article reported a large area growth of p-WSe_2 and studied its electrical properties using the same CVD technique.[31] A new way toward heightening the performance of the device using TMDC's material is doping either by plasma doping[6], superficial charges relocation doping[7] or by surface functionalization[8]. Before TMDC's doping technique was successfully applied on carbon nanotubes (CNT's) using different dopant. In context to dopant Benzyl Viologen (BV) for n-type and Gold Chloride ($AuCl_3$) for p-type are the most favorable dopant using now a days. Biswas et al. successfully stated p-n junction in its article achieved by doping one part of the single wall carbon nanotubes (SWCNT's) with Benzyl Viologen (BV) with different doping concentration.[32] Similarly Kim et al. showed the interaction of Gold Chloride ($AuCl_3$) with CNT's and studied the effect of temperature on CNT's after doping by varying the annealing time.[19] Fig 4 shows the schematic diagram of the interaction of CNT with $AuCl_3$.

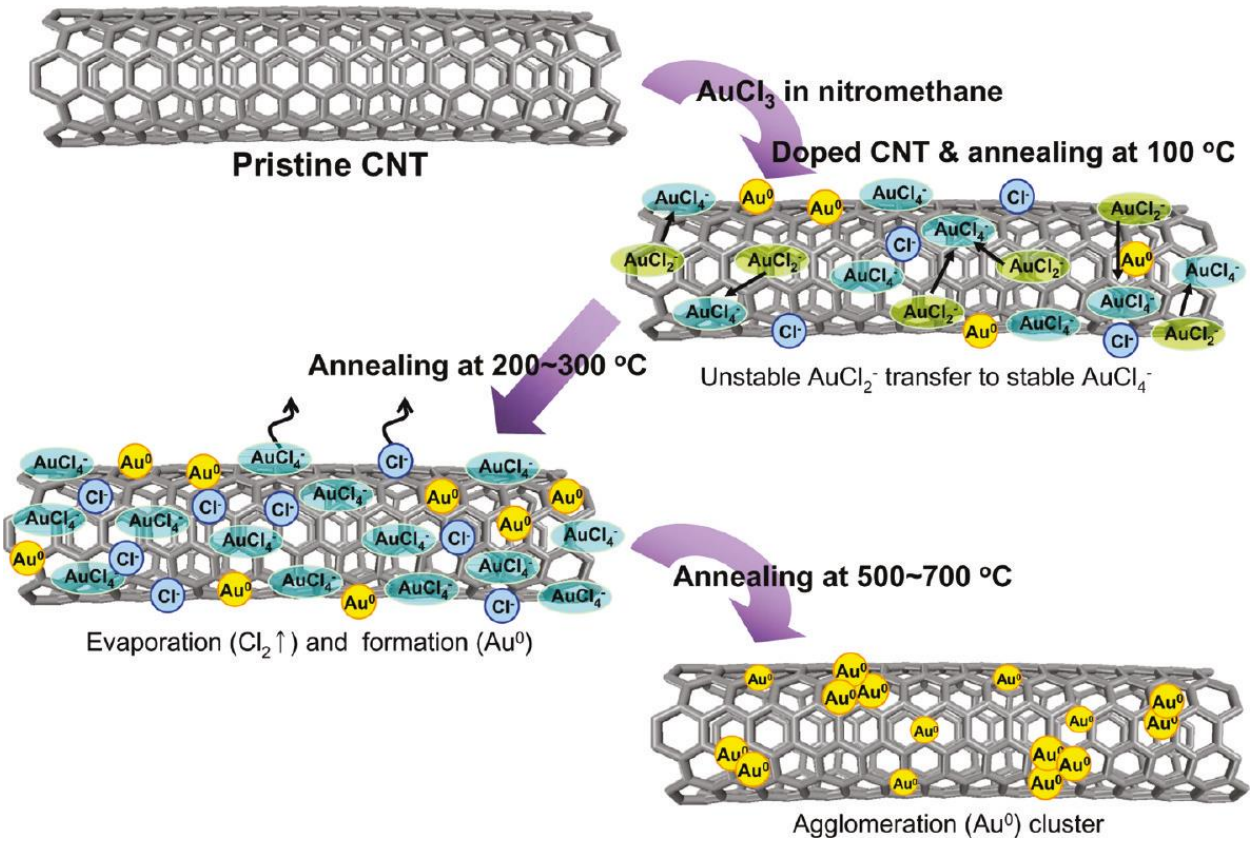

Figure 4: Schematic diagram of doping CNT with $AuCl_3$.[19]

To improve the conductivity of graphene, $AuCl_3$ mix with nitromethane is the most auspicious dopant as reported previously by K K Kim et al. in his article.[20]An effective charge transfer mechanism in MoS_2 has been reported by Ali Javey group using BV dopant showing pronounced permanency in the atmosphere.[7] Fang *et al.* affirmed degenerate n-WSe_2 and p-WSe_2 by treating the contact parts with potassium (K) and Nitrogen dioxide (NO_2) with different disclosure time.[9, 10] Kang *et al.* describe a new method of lightly (Non-degenerate) p-doping of WSe_2 FET by attaching a well-designed methyl (CH_3) group present in octadecyltrichlorosilane (OTS).[1] Chen *et al.* decorated gold Nanoparticles (Au NP) over the surface and ensure p-type WSe_2 FET[11]. Most of the cases 2D material shows degenerate[6-8] state and rarely non-degenerate[1] state after doping with different dopant all of these techniques have many demerits just like low ON state current, low mobility, air stability issues, controlling exposer time and so on. To overcome these kind of situation still there need a lot of research on doping of WSe_2. The most interesting thing in these research works is mobility of electrons and holes increases to some values. Here in this work we also investigate a simple easily process and efficient chemical

way towards an optimized highly doped (degenerate) condition for p-WSe_2 FET using Gold chloride ($AuCl_3$) as a dopant. Which drastically increase the holes injection from Pd to WSe_2 channel and decreases the electron concentration. Our work is much better because of the stability in atmosphere, the mobility is boosted up to a great value, the ON state current changes from 10^{-8} A/µm to 10^{-4} A/µm, the threshold voltage (V_{th}) swing to~75V,the carrier concentration ~10^{15} /cm^2 and a 1000x increase in the conductivity of the device. We also treat WSe_2 with different molar concentration of $AuCl_3$ from 1mM to 40mM to get a perfect, suitable dopant concentration which gives a higher and better performance.

1.1 Basics of Exfoliation:

The process by which a part of material detaches from its source is called exfoliation. All 2D layered materials like Graphene and TMDC's materials have the ability to detach easily from its bulk state due to the week van der Wall force between the stable sheets of 2D materials. Different approaches have been introduced by researchers to exfoliate these materials.

1.1.1 Micromechanical Exfoliation:

The most traditional and widely used technique to exfoliate all 2D materials applied for the first time to exfoliate graphene from graphite. This technique is also named as scotch tape technique because of the use of ordinary daily life scotch tape. In this technique the bulk material is placed on a clean scotch tape and peeled it repeatedly so that monolayers and few layers are separated from its bulk sample. The peeled layers are then transfer onto the substrate by applying some external force as shown in Fig 6. Clean and atomically thin layers could be obtained using this technique.

1.1.2 Chemical exfoliation:

The exfoliation which is carried out in the presence of some chemicals like n-butyl lithium followed by sonication of the solvent is known as chemical exfoliation. In this process powder sample is added to n-butyl lithium in the presence of nitrogen followed by stirring of the sample, filtration and rinsing with hexane, after which water is added to the sample and sonicate for 1 hr to achieve exfoliation of the material.[16]

1.1.3 Liquid Phase Exfoliation:

Liquid phase exfoliation is almost similar to the process of chemical exfoliation but in liquid phase exfoliation the solvent is made to centrifuge after sonication. In this process the powder sample is added to 1-dodecyl-2pyrrolidinone (N12P) followed by sonication for 1 hr after which the mixture were centrifuged at a specific rpm and required time.[17]

2. Experimental details:

2.1. Wafer Cleaning:

Silicon (Si) wafers are available commercially either p-type or n-type (highly doped) with different orientation like (111), (100). Here in this work we used p-type (111) Si wafer with thermally grown 285nm SiO_2 thick layer on the surface of wafer, shown in [Fig. 6(a)], which acts as gate oxide for our device. The resistivity of the wafer is <5Ω-m. Firstly, the wafer was cut into small square pieces of 1x1 inch size using diamond pencil shown in [Fig. 6(b)] and then they were cleaned to remove residue over their surface. Firstly, they were dipped into acetone followed by sonication for around 10 minutes [Fig. 6(c)].After treating with acetone the samples were immersed into isopropanol alcohol (IPA) followed by sonication for 10 minutes [Fig. 6(d)]. Next step is to treat the samples with strongly acidic solution i.e. piranha (H_2SO_4:H_2O_2, 3:1) for about 15 minutes to remove further organic residues from the surface of substrate [Fig. 6(f)]. Before putting the sample into piranha solution, the samples were dried using NO_2 to avoid reaction of solvent (Acetone or IPA) with piranha [Fig. 6(e)]. The final step includes rinsing of sample with deionized (DI) water [Fig. 6(g)] followed by drying with NO_2.

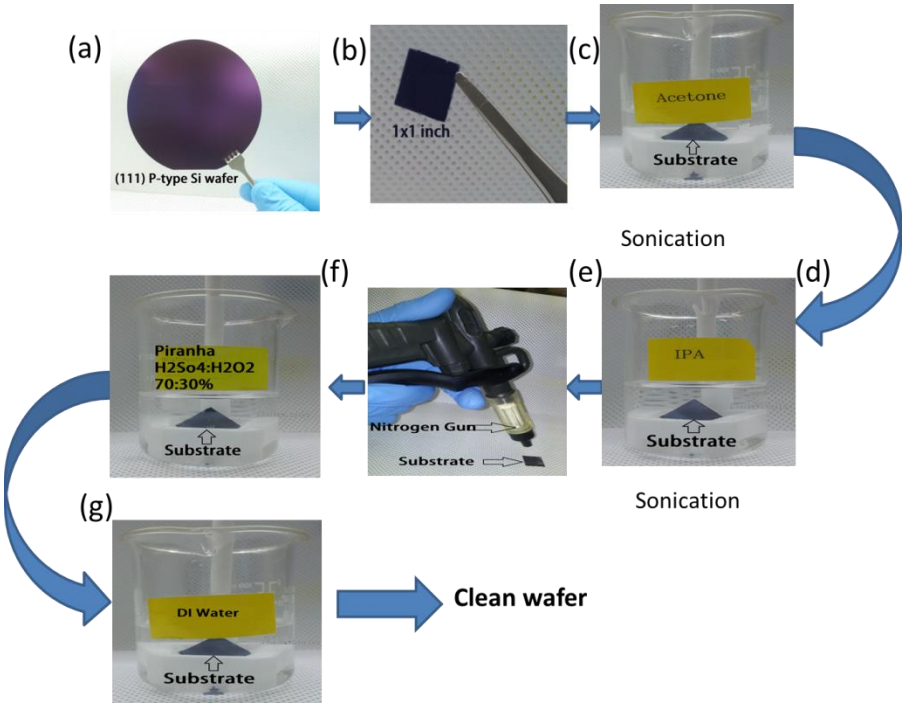

Figure 5: The cleaning process of Wafer. **(a)** Sample of 111-oriented, highly doped p-type of Si-Wafer **(b)** The cutted 1x1 wafer **(c)** Sample dipped into acetone **(d)** Sample immersed into IPA **(e)** Drying of sample with nitrogen gun **(f)** Sample in the piranha solution **(e)** Sample in DI water **(f)** Drying with nitrogen gun.

2.2. Exfoliation:

Exfoliation of 2D and TMDs materials are carried out in a different ways i.e. mechanically [15]or chemically[16, 17]. Here we are using the scotch tape technique (mechanical way) to exfoliate WSe_2. First a small flake of bulk WSe_2 (commercially obtained from Nano surf) was placed on the tape and it is repeatedly peeled to get monolayer or few layers from its bulk WSe_2 [Fig. 7(b, c)]. The cleaned substrate was put upside down on the tape to transfer the exfoliated WSe_2 onto the substrate [Fig. 6(d)]. To ensure better adhesion of WSe_2 with substrate, a vial was smoothly moved across the tape for 1 minute [Fig. 6(e)]. Then after, the substrate was slowly and gently detached from the tape [Fig. 6(e)] and finally, it was rinsed by acetone to remove the tape residue from the surface as shown in Fig. 6(f).

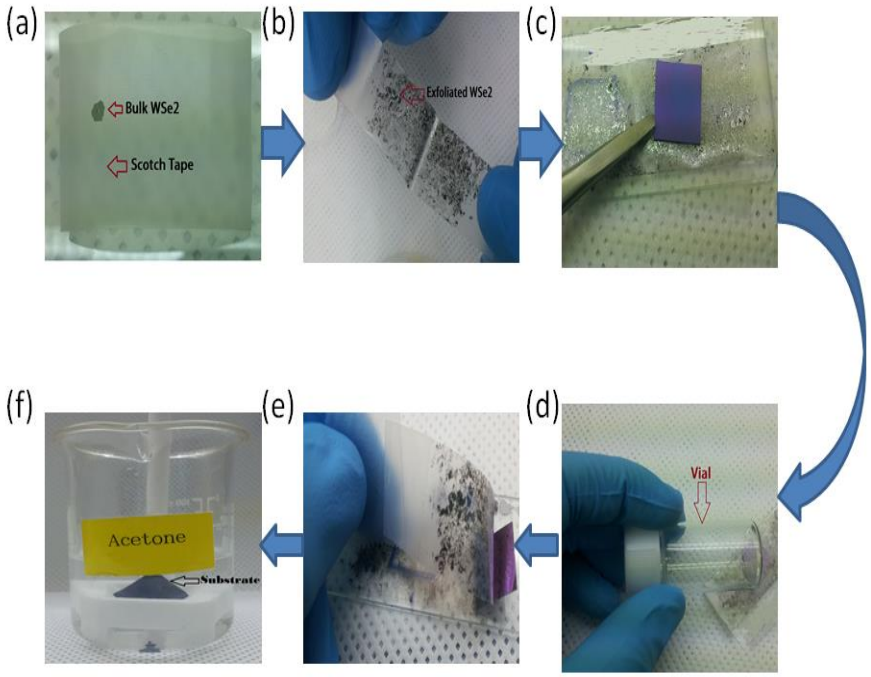

Figure 6: The Process of exfoliation. **(a)** Bulk material on the scotch tape **(b)** The exfoliated material on scotch tape. **(c)** Upside down view of the clean sample on scotch tape to transfer the material **(d)** Rubbing over the surface of substrate using vial to ensure better contact between the exfoliated material and substrate. **(e)** Detaching of substrate from the substrate **(f)** Substrate in acetone for removal of residues.

2.3. Optical Microscope (OM) and Atomic Force Microscopy (AFM) image:

Optical microscope was used to confirm the transfer WSe_2 and the desired flake was selected. The thickness of the flake was confirmed by AFM. Here in our work the focus was to use flake having a thickness between 4~12nm. The Fig. 7(a) shows the OM image of the exfoliated few layered WSe_2flake as shown in Fig. 7(b). AFM image of the final device with the same flake of WSe_2 and the bright yellow broad line shows the "Pd" electrodes which act as a source and drain. Fig. 7(c) shows the measured thickness of the flake from the AFM image. The Red cursor is used to select an average area and the green cursor is used to calculate the thickness of the specific point. The difference between the flake and the substrate in vertical direction gives us the thickness of the flakes. As it is shown in Fig. 7(c) the below line indicates the substrate and the upper line indicates the height of the flake from the substrate. And from the numerical values below the "Y" value is ~12nm which means our flake has a thickness of ~12nm.

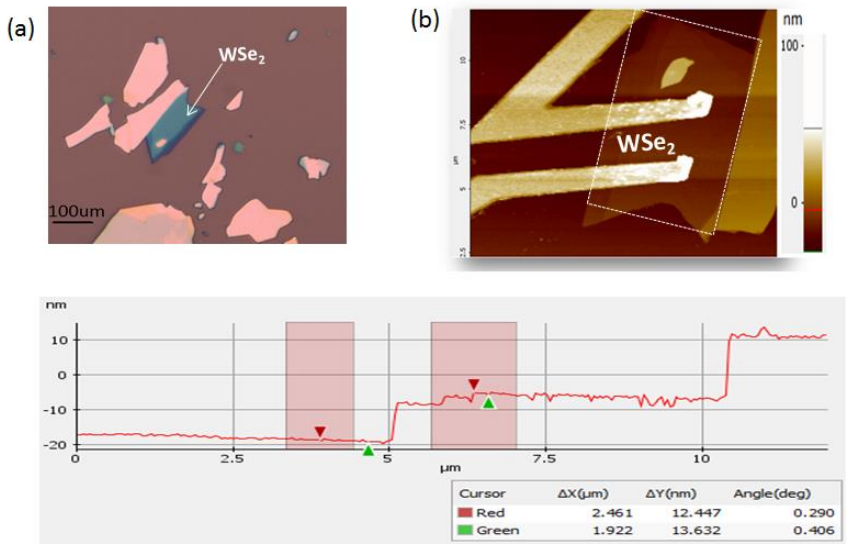

Figure 7: **(a)** OM image of WSe_2 flake. **(b)** AFM image of same flake along with metal electrodes **(c)** AFM data to measure flake thickness.

2.4. PMMA Coating and Drawing Align Marks:

After finding the specific exfoliated flake the position of the flake was determined using OM by simply drawing the "X" and "Y" line from the flake to the closest edge of the substrate. Polymethylmethacrylate (PMMA) A4 was spin coated on the surface of the substrate using spin coater with a rotation of 4000rpm for 60 sec followed by annealing for 90sec with a temperature of 180^{0}C [Fig. 8(a, b)]. The substrate was then cool down and PMMA A6 was spin coated with the same recipe of rotation and backing followed by cooling of substrate [Fig. 8(c, d)]. Now the substrate is ready for align marks. The align marks were drawn on the selected flake using Electron Beam Lithography (EBL) with CAD file as reference [Fig. 8(e)].The substrate was then develop for 1 minute in a mixture (Developer) of IPA: DI water (3:1) [Fig. 8(f)] followed by rinsing with IPA and drying [Fig. 8(g, h)].

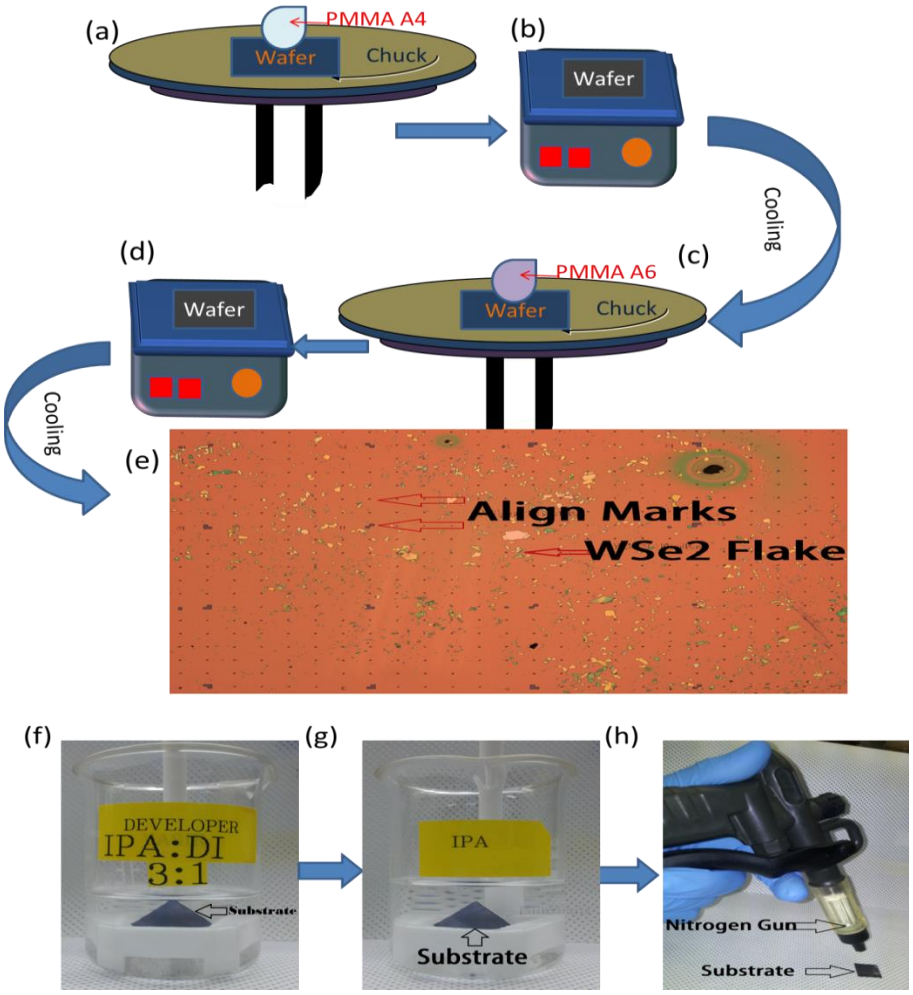

Figure 8: Coating process and drawing align marks. **(a, c)** Coating of PMMA A4/A6 with 4000 rpm **(b, d)** Annealing of the substrate at 180 ^{0}C **(e)** Drawn align marks on the substrate through EBL **(f)** Developing of the sample in a mixture of IPA: DI (3:1) for 1min **(g)** Rinsing of the substrate with IPA for at least 15sec **(h)** Drying of the sample using nitrogen gun.

2.5. Electrode Design and Deposition of Metal:

Before designing of the electrodes pictures of the flake with align marks was taken using OM with different magnification i.e. 2.5x, 10x, 50x, 100x and align all the pictures in ascending order with the design in the Computer-aided Design (CAD) LT 2000 software[Fig. 9(a,)]. After that the desired electrodes are designed on the aligned pictures [fig 9(b)]. Etching was carried out after designing electrodes using EBL followed by developing in developer for 1min rinsing with IPA and drying [Fig. 9(c, d)]. The desired material for the metal electrode was deposited by Electron Beam Deposition (EBD) process in ultra-high vacuum condition [Fig. 9(e)].

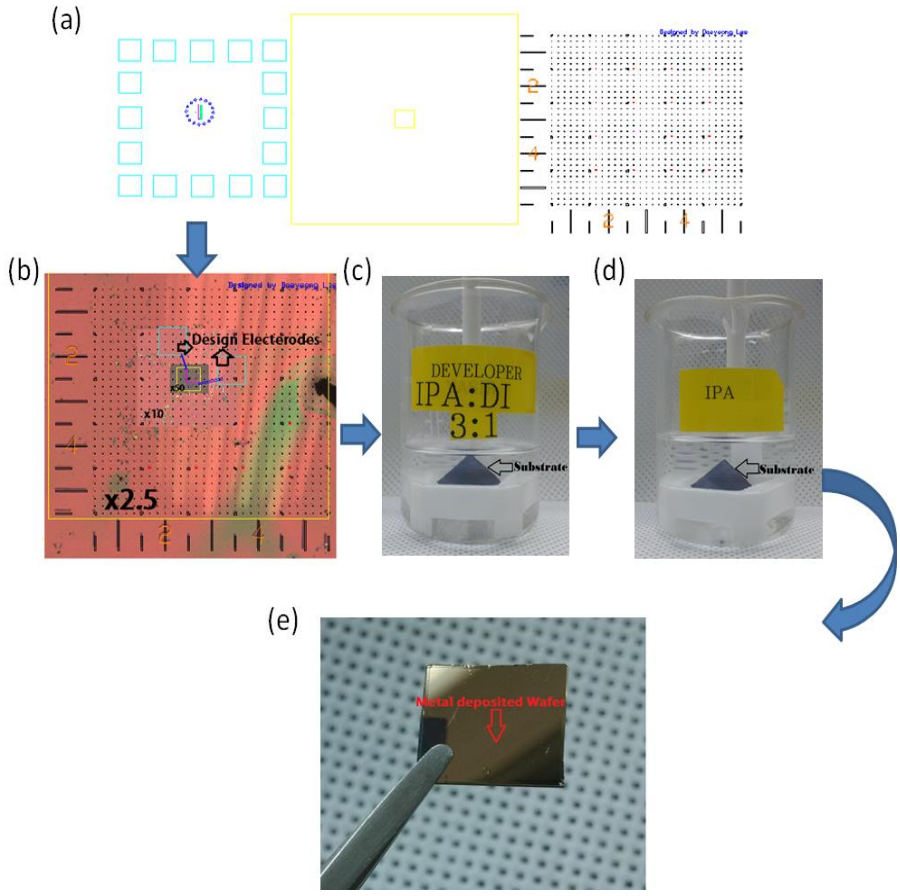

Figure 9: Electrode Design and deposition of metal**:(a)** Built-in Computer-aided design file **(b)** Align pictures with CAD file and the desired electrodes **(c , d)** Developing of the substrate and rinsing with IPA **(e)** Deposited metal on the surface of the substrate.

2.6. Lift-off and Annealing:

After the deposition of metal [Fig. 10(a)], the substrate was kept in acetone for 2-3 hrs to lift-off the excessive metal from the surface of the substrate followed by drying with nitrogen [fig 10(b, c)]. Now the device is ready for measurement. To remove any organic or PMMA residues from the surface of device annealing was carried out using Rapid Thermal Annealing (RTA) in a vacuum of 5mTorr [Fig. 10(d)] with a flow of fuming gas (mixture of Ar/H_2)around 30 sccm . The temperature was maintained at 250 ^{0}C for 2 hrs. The use of annealing help in improving the performance of the device by removing any atmospheric moisture, minimizing the dangling bond at the surface of the material and also the scattering phenomena at the surface is decrease at some extent.

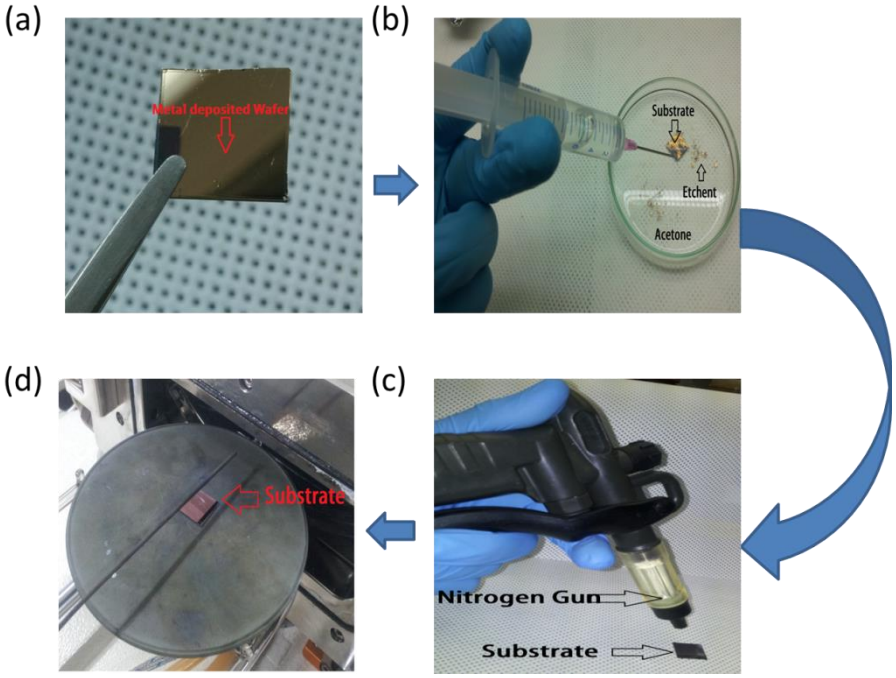

Figure 10: Lift off and annealing. **(a)** Substrate with deposited metal on the surface **(b)** Substrate in acetone for removal of excessive metal from the surface of the substrate **(d)** Drying of the sample using nitrogen gun **(d)** Sample on the RTA stage for annealing at 250 ^{0}C for 2hrs.

2.7. Dopant:

Here in this work we are using $AuCl_3$ as a p-type dopant mix with acetonitrile. The dopant was made by using a simple schlenk line setup. First acetonitrile was poured in a vial with a spin bar and covered the vial with a sipta and tape so that air could not enter into the vial [Fig. 11(a)]. A needle was passed through the sipta and dipped into the acetonitrile for the flow of nitrogen from the acetonitrile while stirring. The vial was kept and holds tightly on the magnetic stirrer and stirring was carried out with a rotation of 300rpm for about 20 minutes. After that degasing from vial containing acetonitrile was done using a common syringe. $AuCl_3$ in powder form (Sigma Aldrich) about 0.034 g was poured into another vial inside the glove box followed by covering the vial. After that the prepared acetonitrile (10 mM) was transfer into the $AuCl_3$ vial using syringe and stirrer it for about 5min followed by making vacuum in the vial [fig 11(b)]. The dopant is now ready and was spin coated on the surface of device with a rotation of 3500 rpm for 60 sec [fig 11(c)]. The substrate was then annealed at 100 ^{0}C for 10min [fig 11(d)]. The spin coating of dopant was done in a glove box because $AuCl_3$ is very sensitive to the environment.

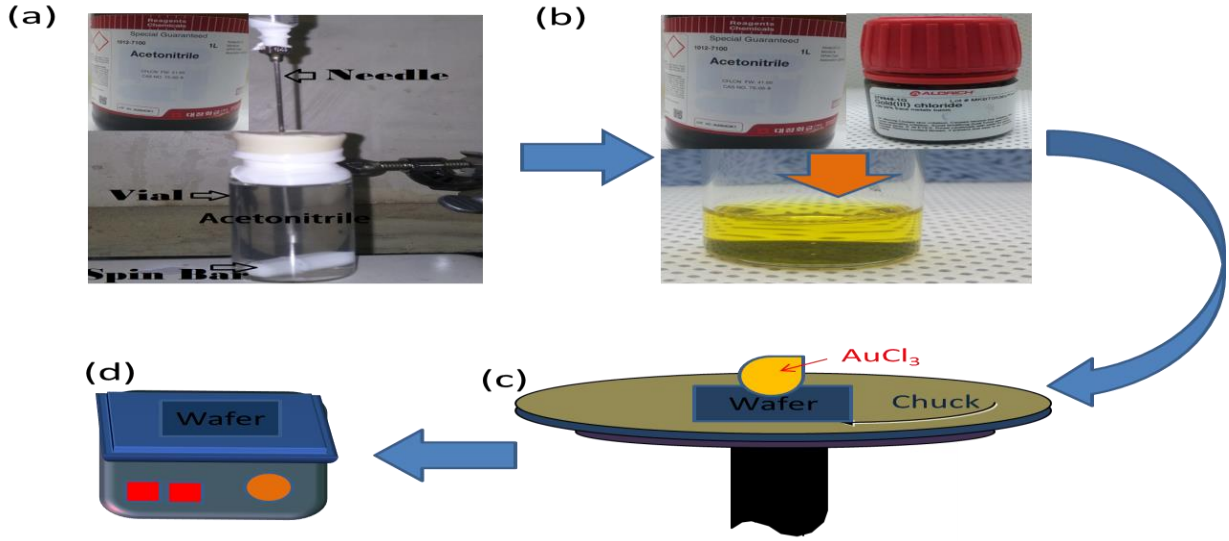

Figure 11: Doping process through schlenk line setup, **(a)** Stirring of acetonitrile at 300rpm for 20mints. **(b)** Mixture of acetonitrile and gold chloride. **(c)** Spin coating of dopant on the surface of wafer. **(d)** Annealing after spin coating for 10mints at 100^0C.

2.8 Device Measurement:

The device was measured using vacuum probe station before and after doping [Fig.12]. First the device was placed on copper substrate which is used as a back gate for our device. The substrate was then put in the vacuum chamber and before connecting the probes vacuum around 20Torr needs to be made in the vacuum chamber. Here first we will connect the probe for gate and then for source and drain on the device.

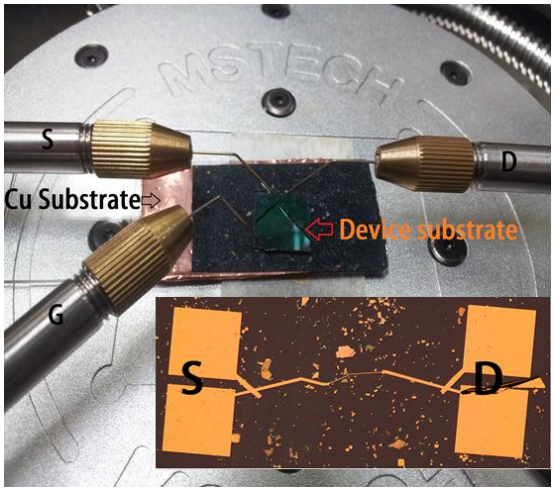

Figure 12: Measurement of the device using four-probe station with device on the Cu substrate and probes are connected via Source (S), Drain (D) and Gate (G).

3. Instrumentations:

3.1 The Optical Microscope:

To select the desired flake of the material on the substrate Optical Microscope (OM) is used as shown in fig 13. With the help of Optical Microscope (OM) we can easily differentiate between the bulk, few layered and monolayer flake of the material.

3.1.1 Operation:

Optical Microscope uses visible light to see the clear image of the sample. To study the sample the objective lens is placed on top of the sample in such way that visible light from the sample enters the microscope at 160 mm focusing point.[33] A bright and extend image can be formed which is clearly seen in the eyepiece of microscope.

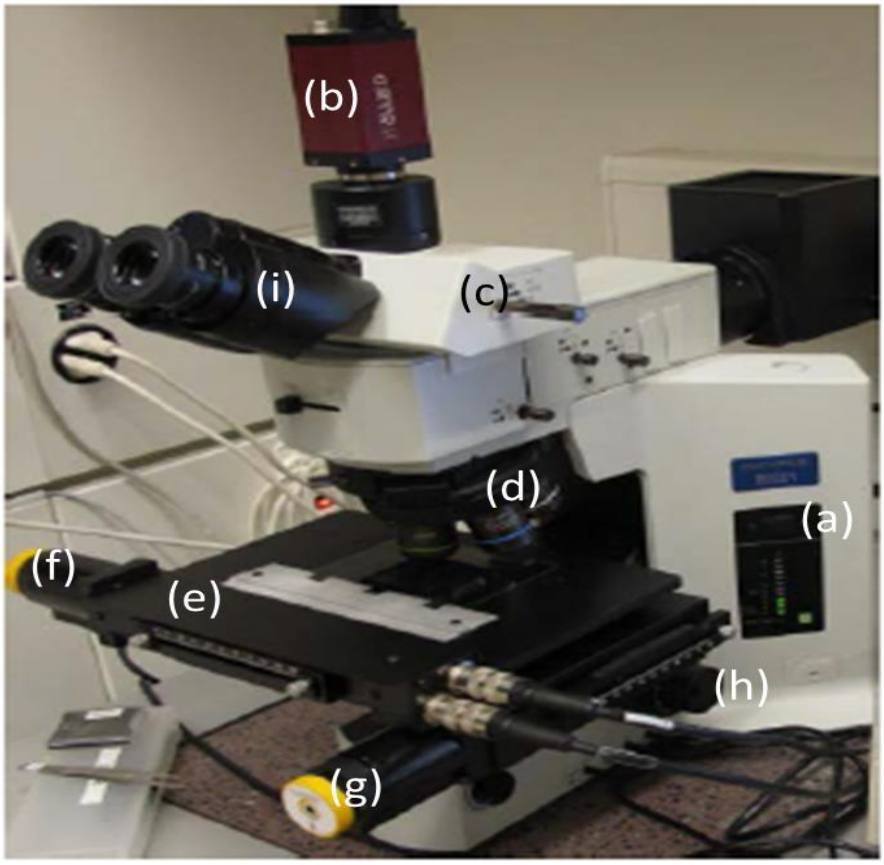

Figure 13: The Optical Microscope (OM) (a) Switch (b) CCD Camera (c) Computer- eye piece switch pin (d) Objectives (e) Sample stage (f, g) Horizontal and vertical caliber knob (h) Magnifying knob.

Fig 13 (a) shows the ON/OFF button of the OM. A "CCD" camera shown in fig 13(b) is attached on top of the OM which captures the image and sends it to the output screen. Fig 13(c) is used to switch between the output screen and eye piece of the OM. To show the images more closely different magnifying glass (Objectives) are used Fig. 13(d) that could be x2.5, x10, x20, x50, x100. Fig 13(e) shows the sample stage on which sample is mounting for observation. The sample stage could be easily move either up and down or from left to right with the help of knobs as shown in Fig 13(f, g). To make the image clear the magnifying glass can be move up and down using knob as shown in Fig 13(h). The eye piece of the OM is shown in Fig 13(i).

3.2 Vacuum Probe Station:

Vacuum probe station is frequently used for the electrical characterization the fabricated device Fig 14. Ultra high vacuum is used during measurement that's why we call it vacuum probe station.

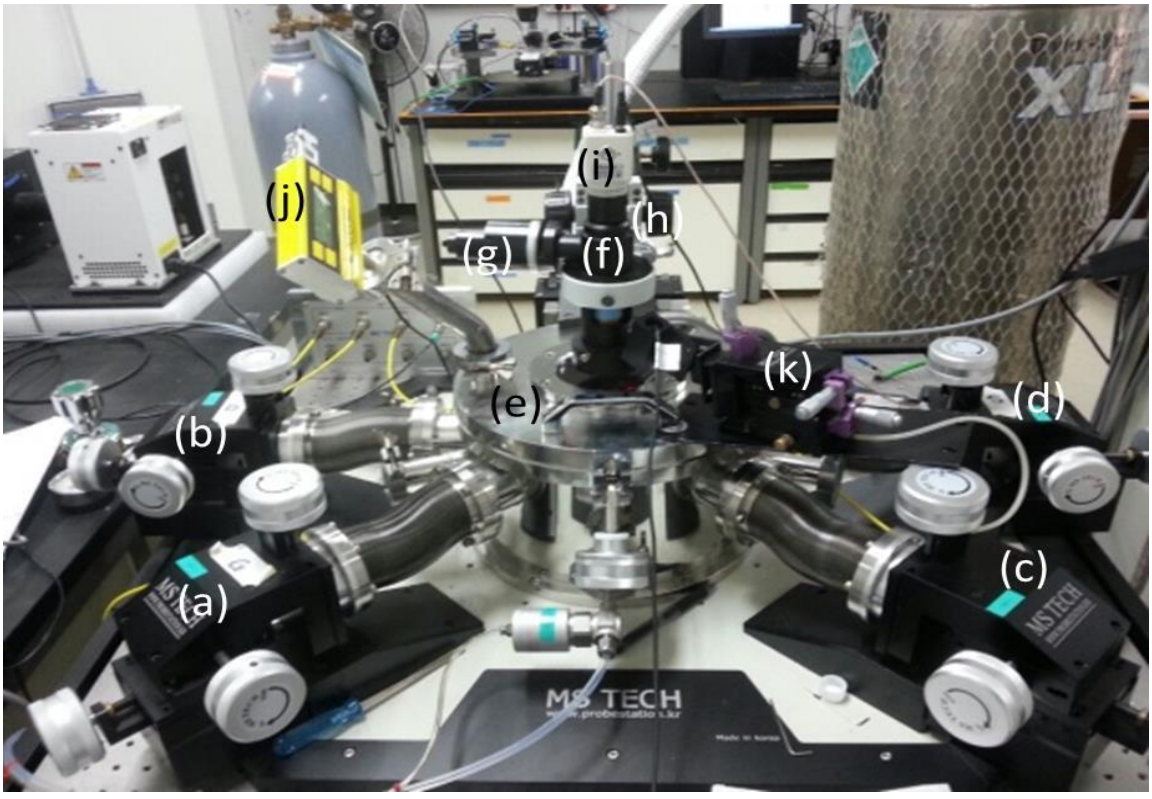

Figure 14: Vacuum Probe Station. (a, b, c, d) four probe aligners (e) Vacuum chamber (f, g) light source and magnifying glass (h) Vertical caliber knob (i) CCD camera (k) Laser source.

The station consists of four probes which are used for connecting as a source, drain and gate etc. with the contact pad of the device. The probes can easily be aligned with the help of these schemers as shown in Fig. 14(a, b, c, d). The device is kept in the vacuum chamber as shown in Fig. 14(e). A light source and magnifying glass having resolution of x100 is attached on top of the chamber to see the clear image of the device Fig. 14(f, g). To move the magnifying glass up and down a knob is used as shown in Fig. 14(h). A "CCD" camera is also attached on the top Fig. 14(i) by which we are capable of seeing a clear and magnified image in the output monitor installed with the station. Fig. 14(j) shows a vacuum meter which measures the actual value of pressure inside the vacuum chamber. A laser source can be used to measure the optical response of the device as shown in Fig. 14(k).

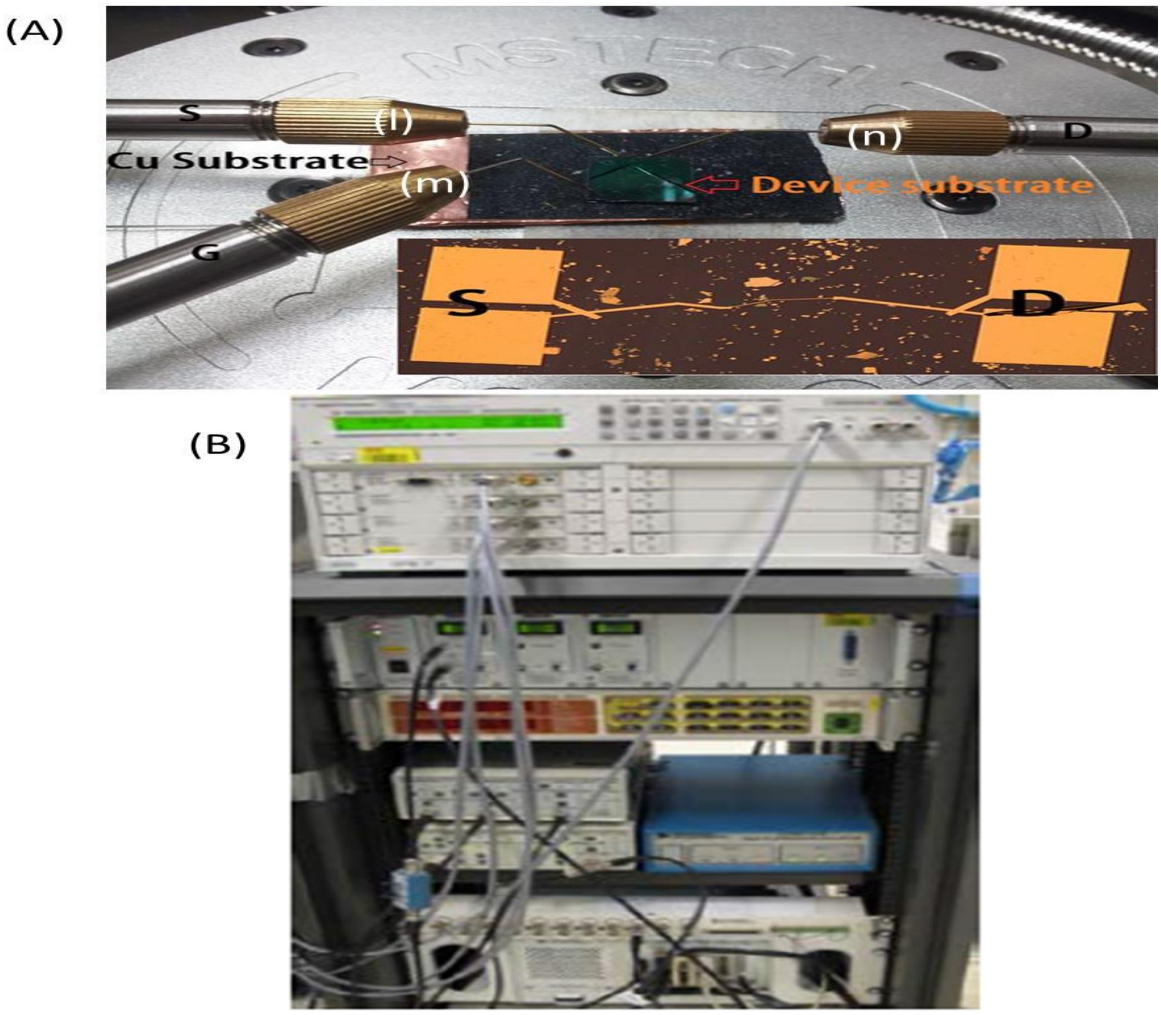

Figure 15 (A) Inside view of the vacuum chamber (l) source tip (m) gate tip (n) drain tip (B) Analyzer.

Fig. 15(A) shows the inside view of the vacuum chamber in which probes are clearly can be seen connected as a source, (l) gate (m) and drain (n) with the device which is mounted on a Copper (Cu) substrate. Fig. 15(B) shows an analyzer to control the whole station and vacuum of the probe station.

3.3 Electron Beam Lithography (EBL):

To draw the pattern of electrodes and align marks a very high beam of electrons can be used to etch the coated PMMA from the surface of the substrate using Lithography technique, the whole process we call "Electron Beam Lithography" Fig. 16. In the EBL the beam of electrons is so narrow that it is capable of drawing a very precise pattern.[23, 24] The sample is mounted in a high vacuum chamber, the area is to be specified and controlling of electrons beam is done using the attached setup.

Figure 16: Electron beam lithography (EBL).

3.3.1 Working Principle:

The working principle of the EBL is such that an electron beam is generated from the electron gun passes from the alignment coil which helps in aligning the beam of ejected electron and hence the electrons are controlled from scattering. The use of condenser lenses helps in focusing the beam of electrons at a specific point when the beam passes through it. Blanking plates are added to the instrument which is used for shrinking or weakening or we can say turning ON/Off the beam where there is no need of it. The beam of electrons after passing through all the lenses and plates hit resist spin coated on the substrate and scan the substrate for drawing the pattern. Two types of scanning can be done by this instrument i.e. either raster scanning or vector scanning. In raster scanning the beam chronologically scan all part of the substrate while in vector scanning the beam scan the desired area i.e. the beam moves from one point to another. The schematic internal diagram of the EBL is shown in Fig. 17.

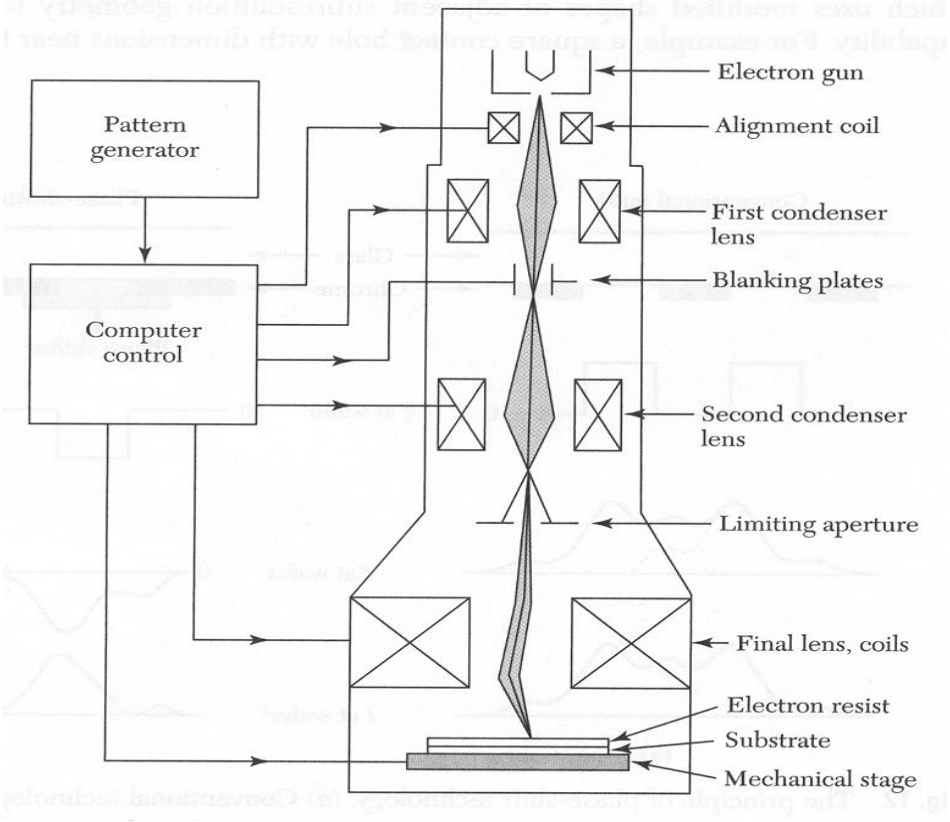

Figure 17: Schematic internal diagram of EBL.[34]

3.4 Electron Beam Deposition (EBD):

To deposit materials (gold, silver etc.) on the surface of the substrate to make the electrodes permanent of desired thickness “Electron Beam Deposition” is used as shown in Fig. 18. The whole process is done under a very high vacuum inside EBD and the instrument is placed in a clean room to avoid any dust particles. EBD uses a high energetic electron beam produced by thermal emission or field emission. The working principle of EBD is such that electron beam from the filament allow to interact with the material using electromagnetic phenomena, magnetic field is applied to straightening the beam from the filament to the material, while electric field helps in navigating the beam over the specified surface. The Kinetic energy of the electrons is converted to thermal energy upon interaction with the material which helps in sublimation of the material from the source and is fade away, as a result a thin layer is deposited on the surface of the substrate followed by lift off and annealing of the sample.[24,35]

Figure 18: Electron beam deposition (EBD).

3.5 Rapid Thermal Annealing (RTA):

To enhance the performance of the device i.e. the electrical properties or remove any residues/moisture from the surface of the substrate annealing is to be carried out in a vacuum and in the presence of Nitrogen gas. The instrument used for annealing in this project is "Rapid Thermal Annealing (RTA)" Fig. 19 in which the sample is annealed with a temperature of 250 ^{0}C for 2 hours.

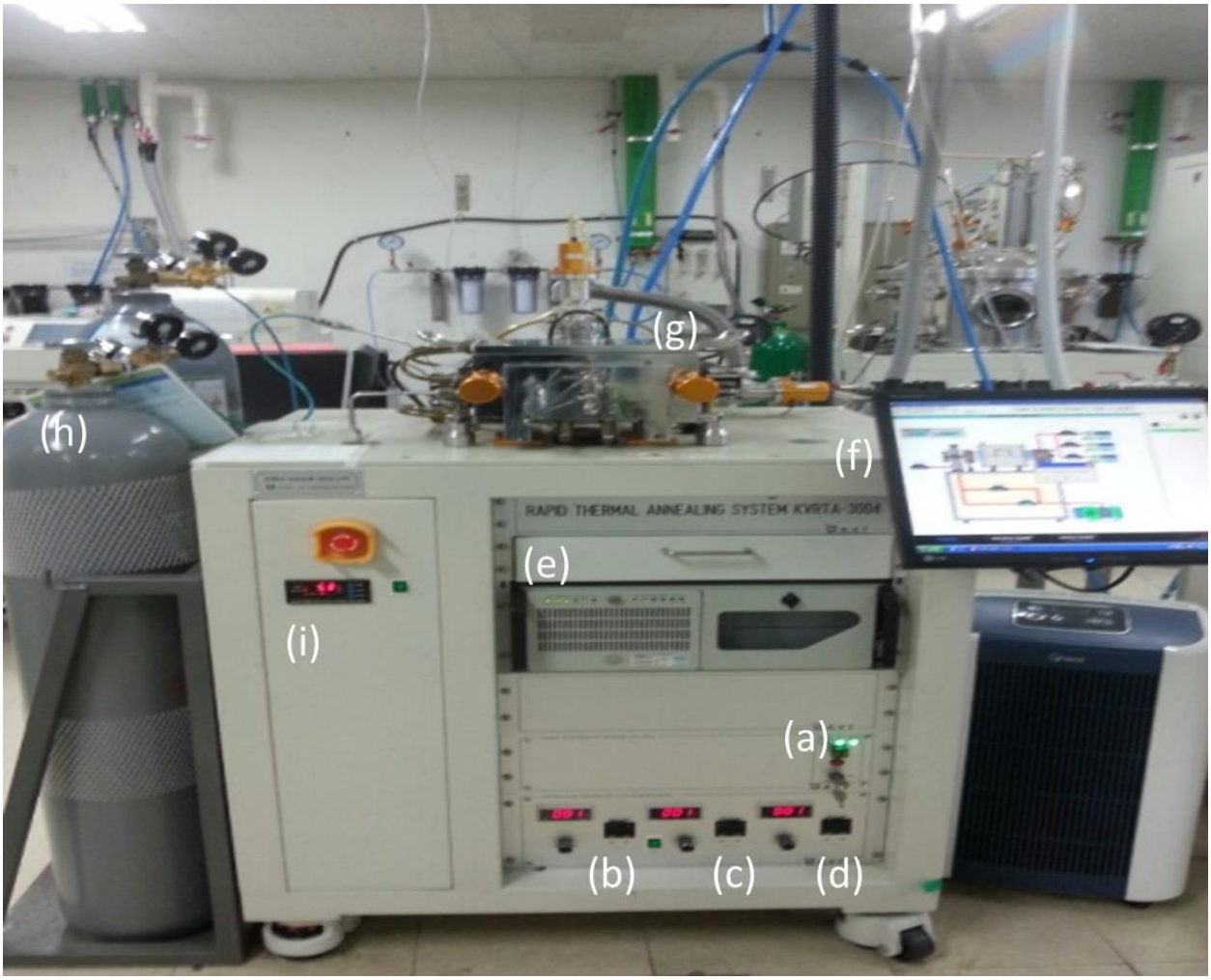

Figure 19: Rapid Thermal Annealing (RTA). (a, b, c, d) Starting knobs (e) Computer (f) Output screen (g) Annealing chamber (h) Gas cylinder (i) Meter.

RTA is mostly used for annealing of Silicon substrate up to 1000 ^{o}C with in few seconds followed by gradually cooling down of substrate to minimize the breaking of wafer.[36] A Neon lamps or laser lamps are connected in series inside the vacuum chamber for getting such a high heating rate. RTA covers a wide range of application related to the fabrication and processing of semiconductors like dopant stimulation, thermal corrosion, metal reflection and chemical vapor deposition (CVD). [36, 37] To turn ON RTA a switching key needs to be rotate as shown in Fig. 19(a) then turn ON all the three knobs Fig. 19(b, c, d) as a result the machine will be automatically starts. A computer is connected with the RTA Fig. 19(e) by which we can give our desired recipe using software installed in the computer. The flow diagram of all the gas pipe lines connected with the RTA is to be controlled from the output screen as shown in Fig. 19(f). Fig. 19(g) shows the annealing chamber first you have to evacuate all the gases so that you can easily put your sample inside the chamber. Nitrogen gas cylinder is connected with RTA as shown in Fig. 19(h). To start annealing you must have to be assuring that the pressure inside the chamber is less than 10mbarr shown in the digital meter Fig. 19(i) but it will increase when you open the valve of Nitrogen gas.

3.6 Glove Box:

Doping of the sample must be carried out inside the glove box because Gold chloride ($AuCl_3$) is highly reactive with the oxygen present in the atmosphere. Fig. 21 shows the image of simple glove box.

Figure 20: Glove Box (a) Small vacuum chamber (b) Pressure monitoring screen.

To use the glove box first you have to put sample in a small chamber Fig. 20(a) and then make vacuum inside the chamber by repeating the process of air flow inside the chamber for at least three times with duration of 10 mints. The pressure and light inside the box is to be controlled from the output screen attached with the box as shown in Fig. 20(b).

3.7 Schlenk line:

The authentic way of making dopant is by schlenk line process in which a number of pipe lines are connected in series having two ends one is connected with the vacuum pump for making vacuum inside the vial and the other with nitrogen gas because the process is carried out in the presence of nitrogen gas Fig. 21.

Figure 21: Schlenk line Process.

3.8 Atomic Force Microscopy (AFM):

Atomic force microscope has the ability to measure the roughness of the surface, the microfabrication of the sample, identification of the atoms at the surface and also study the physical changes ascends from the ordering of the atom at the surface.[38] A tip is connected to a movable cantilever which is able to move in x-y directions. To study the surface the tip is allowed to contact with the surface in a different mode i.e. contact mode, non-contact mode and tapping mode. To measure the thickness of the desired flake atomic force microscopy (AFM) is used. Before measuring the thickness of the flake encircles the position of the flake so that it could be easily located for characterization. The parameters of the AFM are to be controlled from installed software as shown in Fig. 22(a). Fig. 22(b) shows the output monitor in which a clear image of the tip could be seen send by a CCD camera installed on the top of the tip of AFM.

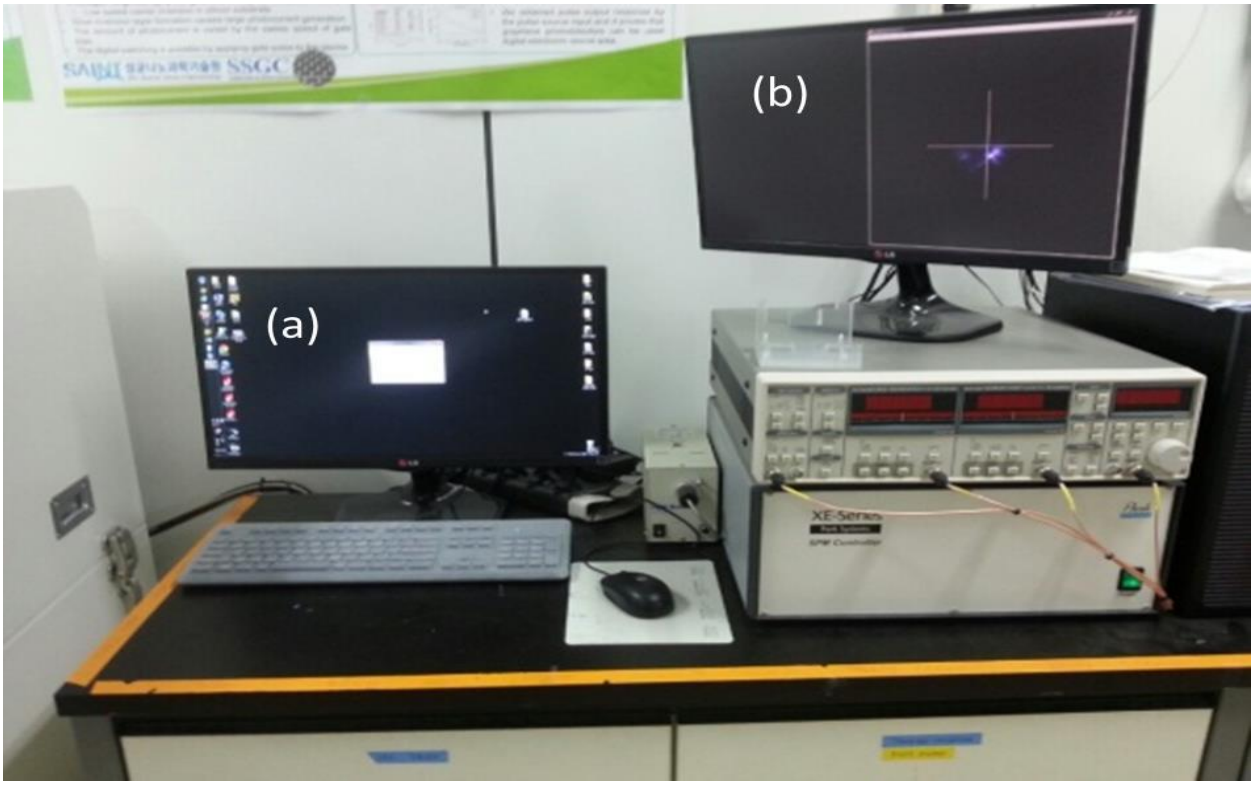

Figure 22: Atomic Force Microscopy (AFM) (a) Parameters controlling monitor (b) Output monitor connected with CCD camera.

4. Results and Discussion:

4.1. Electrical measurement:

Fig. 23 shows the schematic diagram of our back-gated field effect transistor (FET) devices fabricated by electron beam lithography (EBL) technique. Few layers WSe_2 flakes are gained by traditional way of micromechanical exfoliation from the commercially purchased bulk WSe_2 on 285nm Si/SiO_2 (Extremely p-doped) substrate. The pattern of desired electrodes (Source/Drain) is designed and draw by using CAD file and EBL keeping the length (L) and width (W) of the channel at 2.78 µm and 2.91 µm. "Pd" is the high work function material with respect to WSe_2, who's work function is ~4.6eV used for source and drain are deposited through Electron Beam Deposition (EBD) having thickness of 20nm followed by lift-off to remove excessive material. The purpose of using high work function "Pd" as a metal contact is to get an increment in the hole carrier density and a decrease in the electron carrier density in WSe_2 FET. The use of high work function material like Pd, Pt lower the Fermi level towards valence band while its counterpart i.e. low work function material like Ag, Cr and Al moves the Fermi level towards the conduction band as a result of change in Schottkey barrier which in turn modulates the carrier injection from the metal to WSe_2.

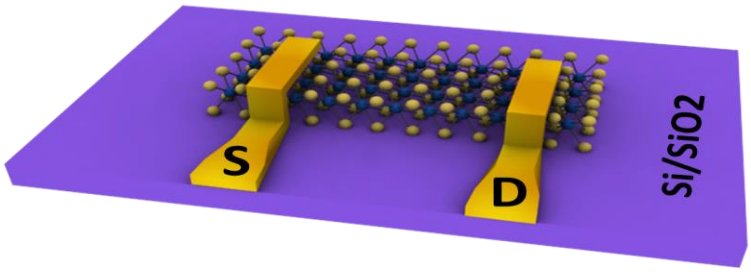

Figure 23: 3D image of the back gated field effect transistor.

Fung *et al.* reported in his paper that Pd is considered as one of the best contact material for gaining p-type WSe_2 FET.[11] In this work our device shows an ambipolar behavior with both the hole and electron density. To get a highly p-type WSe_2 FET, we are using a chemical way of

doping with Gold Chloride ($AuCl_3$) mix with Acetonitrile (ACN) in a ratio of 0.034g: 10mM as a chemical dopant. As a result the electron concentration in an ambipolar $WSe_2$was decrease and the hole concentration increases showing a clear and prominent p-WSe_2 FET.

The electrical measurements of the device are carried out before and after doping at a room temperature in a vacuum chamber with a 20 m barr. The output characteristic curve i.e. I_{DS} -V_{DS} at different V_{BG} and transfer characteristics curve i.e. I_{DS} -V_{BG} at different V_{DS} are obtained as shown in Fig.24.

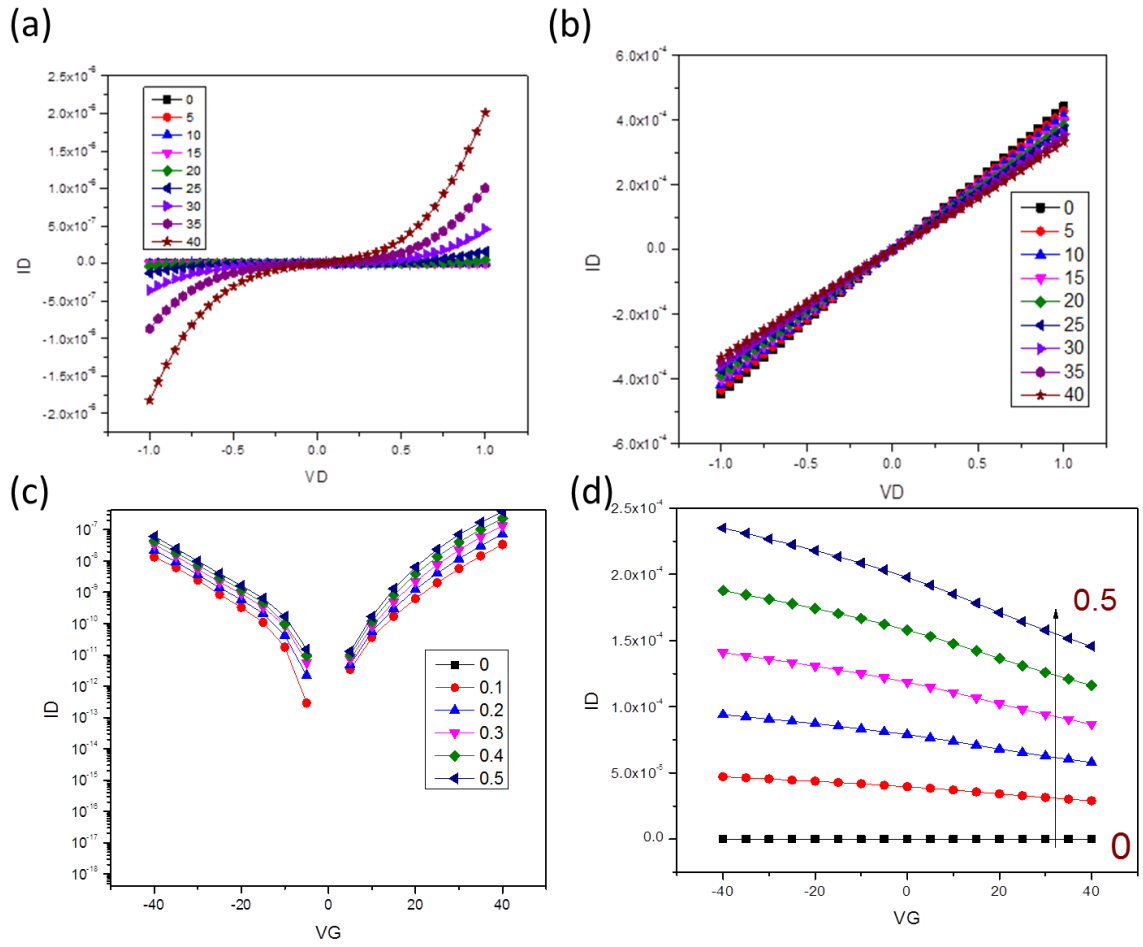

Figure 24:**Electrical results of our device before and after doping.(a, b)** shows the output curve at different V_g, before and after doping respectively.**(c, d)** denotes the transfer curve at different V_d before and after doping respectively.

Fig. 24(a) shows the transfer characteristic "I_{DS} -V_{DS}" curves at different gate voltages "V_{BG}" values before doping and it is clearly shown from non-linear curve that our device has a high resistance Schottkey behavior with "Pd" contacts. Due to high Schottkey barrier and contact resistance the possibility of crossing electron/hole through the barrier is very low. But after

doping with $AuCl_3$, the electrical behavior is totally changed from Schottkey to ohmic-like, as shown in Fig. 24(b) and it correspond to a very low contact resistance between Pd and WSe_2. Fig. 24(c) shows the output characteristic "I_{DS} -V_{BG}" curve at different drain voltages (V_{DS}) and from the graph it is obvious that our device shows ambipolar behavior. But as we treat the sample with $AuCl_3$ dopant, the device ambipolarity is changed to unipolarity showing only p-type behavior as shown in Fig. 24(d). The ON/OFF ratio concerned with our device also shows the superiority of $AuCl_3$ with other dopant as previously reported. Here in this work the value of "ON" current at higher negative value is significantly increased from 10^{-8}A/μm to 10^{-4}A/μm after treating with $AuCl_3$. It also shows the device uncontrollability on gate voltage i.e. the increase or decrease in gate voltage did not affect the drain current of our device.

The hole mobility "μ_h"of the device was measured from the I_{DS} -V_{BG} characteristic curve before and after doping using the relation$\mu = \frac{1}{C} \times \frac{d\sigma}{dV_{BG}}$, where C is the capacitance of oxide and for 285nm thick SiO_2, its value is C=1.09x10^{-8} F/cm^2, V_{BG} is the gate voltage, σ" is the total device conductance and is equal to $\sigma = \frac{L}{W} \times \frac{I_{DS}}{V_{DS}}$ with L *and* W are length and width of the channel respectively. Keeping the drain voltage (V_{DS}) at 0.5 the calculated mobility after doping shows surprisingly increment up to149 cm^2/V.s from 0.26 cm^2/V.S at 10mM concentration of $AuCl_3$ which is the highest mobility we obtained at this concentration as compare to the previous reported value ~100 cm^2/V.S using gold nanoparticle (AuNP) by Chen *et al*[12].It also indicates that how efficient our dopant is as compare to other dopant techniques. We also measure different devices by varying the molar concentration of $AuCl_3$ dopant from 1mM to 40mM to check that at what concentration our device gives a high and more stable performance. From the results we obtained, at 10 mM concentration the P-WSe_2 FET gives higher value than that of the other concentrations. Fig. 25(c) shows the graph which is drawn between the hole mobility and the concentration of $AuCl_3$. In this work as we increase the concentration of dopant from 10mM up to 40 mM the hole mobility of our device start degrading.

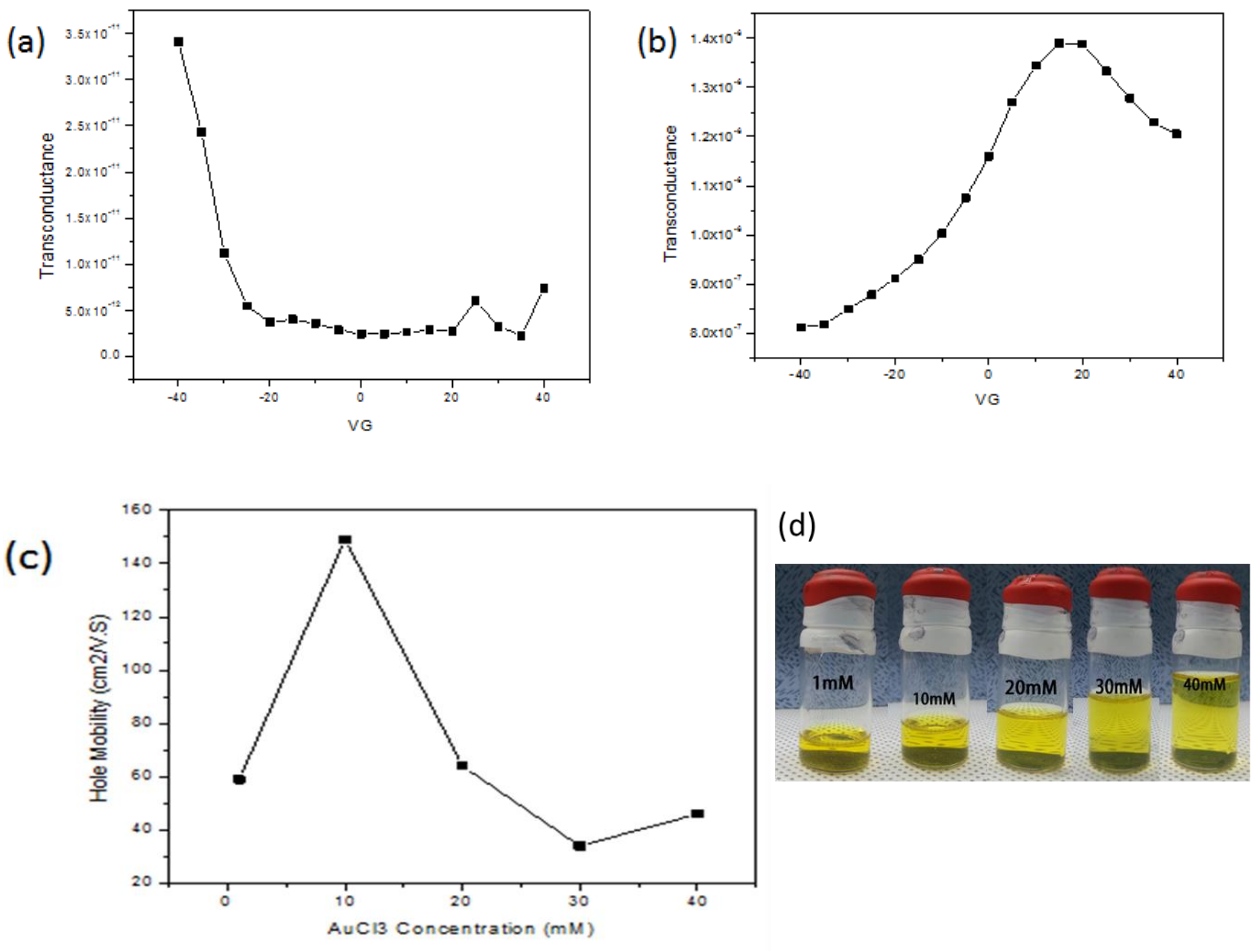

Figure 25: **The doping effect on device mobility**. **(a)** Graph of the transconductance with respect to gate voltage before doping showing a decrease in slope as V_g moves toward negative value. **(b)** Shows the transconductance after doping with an increase in slop as the V_g value increase positively. **(c)**The calculated mobility with respect to doping concentration after doping showing a higher mobility at 10mM concentration. (d) Images of different dopant concentration

To support the argument about the increment in the mobility after doping we plot the transconductance. Fig. 25(a) shows the transconductance of our device with different gate voltage (V_{BG}) before doping and from the graph it is clearly witnessed that the slope is negative and going to decrease as the value of gate voltage moves towards positive value which is a cause of getting low mobility. Whereas Fig. 25(b) shows that the value of slope is not even positive but also it increases as the value of gate voltage shift towards positive value due to which we can get a higher mobility. Here in this case the mobility is not the real mobility (Contact resistance (R_c) included). Generally, the mobility of the device decreases after doping because of increase in carrier concentration that increases the scattering effect of electron or holes with the lattice. But

here in this case, the doping and mobility trend is opposite i.e. instead of decreasing, it increases. Usually, the Nano device operation is dominated by contacts.[21, 22] Therefore, when WSe_2 device is doped, a more prominent impact is observed at the contacts i.e. the width of the barrier between Pd and WSe_2 is thinned, that lowers the contact resistance as well as the sheet resistance up to a great extent, which dominates over the scattering phenomena in the 2D sheet at the surface. The result of lowering contact resistance and thinning in width of the barrier between Pd-WSe_2 allows holes to inject through the barrier easily from the metal to WSe_2 as a result we can get a higher hole mobility. The decrease in hole mobility at high dopant concentration above 10mM is the result of excessive charged carriers' accumulation near the contact area and increase in charge carrier in the channel as well, in result of that the scattering phenomena, which causes lowering in the hole mobility, is overcome by contact thinning. And this phenomenon is further explained by energy band diagram in Fig. 26.

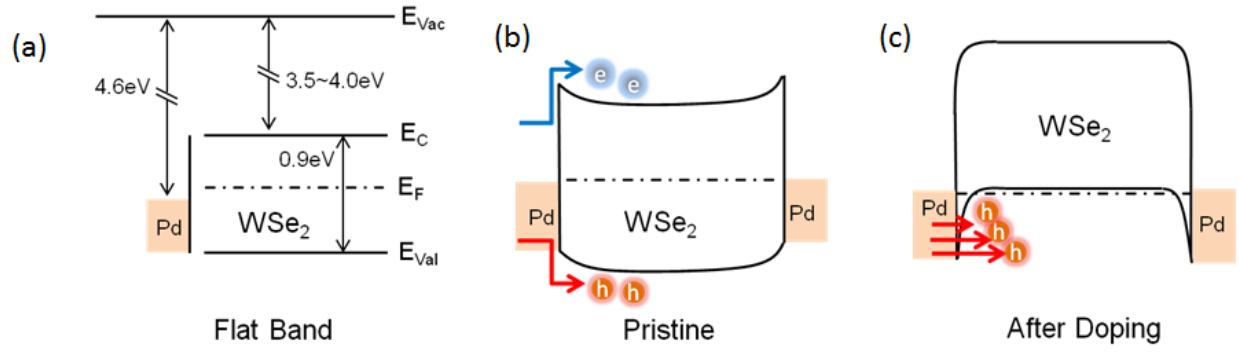

Figure 26: **Energy band diagram of metal-WSe2 device and doping effect**. **(a)**The flat band structure of WSe_2 with Pd contact. **(b)** The band diagram of WSe_2 device after contact is made. **(c)** The band structure after doping with thinning the barrier width near the valance band and the tunneling of hole through the barrier.

In Fig.27 (a) the first diagram shows the flat band structure of WSe_2 with the Pd as a contact material. It also shows the band gap (E_g) and the work function of Pd with WSe_2. Fig 26(b) shows the band diagram of pristine WSe_2 in which the E_f level lies almost between the conduction and valance band. The ambipolarity of WSe_2 is due to the electron-hole pair generated thermionically at the interface and can easily move from source to drain. While in case of doped sample as shown in Fig. 26(c), the (E_f) moves toward the valance band which is feasible for the holes to migrate from source to drain but for electrons at this condition the ratio

to overcome the barrier were very less almost zero so that's why we are unable to get an ambipolar behavior.

The carrier density of the two dimensional sheet (n_{2D}) is calculated from I_{DS} -V_{BG} characteristic curve using the relation $n_{2D} = \frac{I_{DS}L}{qWV_{DS}\mu}$ at V_{DS}=0.5V where q is the charge on electron, μ is the mobility of our device, I_{DS} is the drain current, V_{DS} is the drain voltage and L,W are their respective length and width. From the calculated value it shows much similarity with the previously reported[8, 10] value with a carrier concentration ~1.3x10^{13} cm^{-2} after doping with $AuCl_3$. The calculated value of carrier density (n_{2D}) shows that our doping concentration is around 1.08x$10^{19}$$cm^{-3}$ (after normalizing with thickness of flake) showing a degenerate doping with Fermi level (E_f) goes down the valence band (E_v).

4.2. Doping Process of $AuCl_3$ with WSe_2:

From the last few decades doping is one of the projecting way to improve the performance of operational device on demand. Now a day's different approach of doping have been carried out i.e. ion implantation, plasma, Nano particles and chemical doping etc. Here we are using the chemical way to dope our WSe_2 FET using $AuCl_3$ as a chemical dopant. $AuCl_3$is one of the finest compounds used as a dopant for oxidizing polymers[18], one dimensional Carbon Nano tubes (CNT's) [19] and 2D materials like Graphene [20]. Here we are using acetonitrile as a solvent, because $AuCl_3$ form a neutral coordination when react with acetonitrile instead of making square planer geometry as in the case of nitromethane. [18] Here in our case $AuCl_3$ react with WSe_2 in the following step of reactions, similar to graphene and CNT doping mechanism.[18, 19]

$$2WSe_2 + 2AuCl_3 \longrightarrow 2WSe_2^{+} + AuCl_2^{-} + AuCl_4^{-} \quad (1)$$

$$3AuCl_2^{-} \longrightarrow 2Au^{0}\downarrow + AuCl_4^{-} + 2Cl^{-} \quad (2)$$

$$AuCl_4^{-} + 3WSe_2 \longrightarrow 3WSe_2^{+} + Au^{0} + 4Cl^{-} \quad (3)$$

In the first step $AuCl_3$ react with WSe_2 as a result $AuCl_3$ reduced to Au^3 and Au^1. In the second step the uncoordinated Au^1 further reduced to Au^0 in addition of $AuCl_4^-$ and Cl^- . The reduction of Au^1 is due to the uncoordination with the solvent. Further there may occur the reaction of $AuCl_4$ with WSe_2 to form stable Au^0 particles in the surface of WSe_2 in the presence of large amount of $AuCl_3$. The process of annealing after spin coating of doping can enhance the

performance of device due to the evaporation of Cl^- from the surface of WSe_2 leaving behind a stable WSe_2 structure.[19]

$$WSe2^{+} + AuCl_4^{-} \longrightarrow WSe_{2^-}\, AuCl_4 \qquad (4)$$

In this whole process Au^0 particle plays an important role in the p-type doping of WSe_2. The schematic reactions of $AuCl_3$ with WSe_2 are shown in Fig. 27.

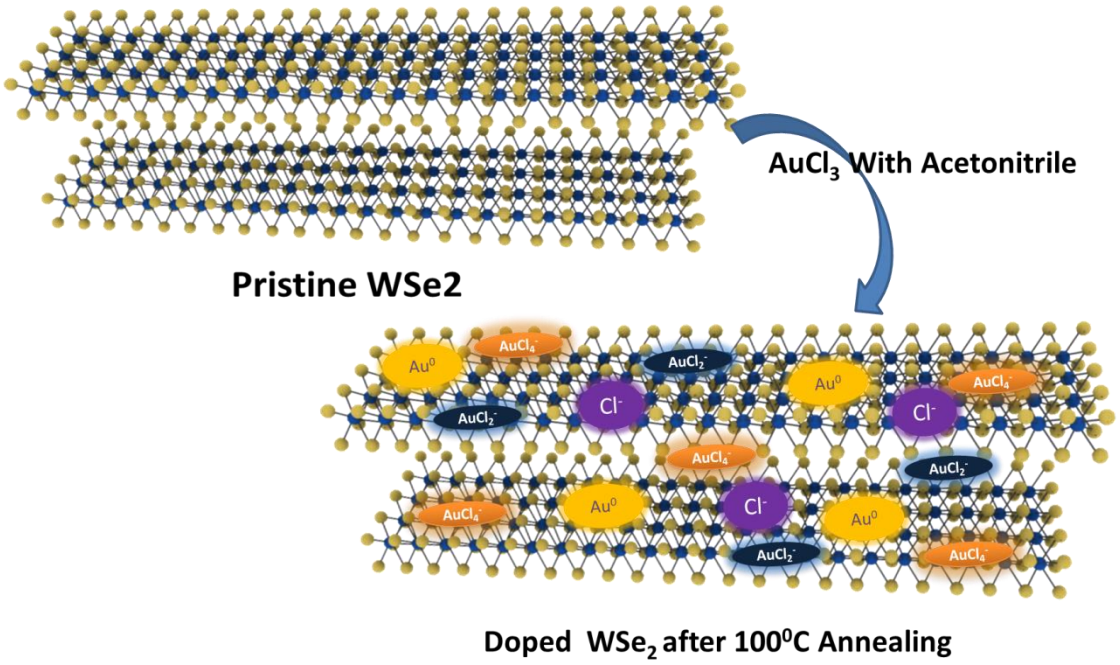

Figure 27: Schematic diagram of doping mechanism of$AuCl_3$ with WSe_2.

Conclusion:

In conclusion we have fabricated a p-type WSe_2 field effect transistor gained by a chemical way of doping using $AuCl_3$ mix in acetonitrile as a dopant. The P-type behavior basically comes from the reduction of Au^{+3} to stable Au^0 particles upon the reaction of $AuCl_3$ with WSe_2. Here Au^0 particles act as an acceptor results in a charge transfer mechanism from WSe_2 at the surface and interface between the layers. The p-type behavior was confirmed from the electrical measurement of the device i.e. the ambipolarity of the WSe_2 changes to unipolarity and a strong change in barrier between Pd-WSe_2 from schottkey to ohmic-like. Besides from this we have also inspected that at 10mM concentration our doping become stable and optimized with a doping level of ~$1.3x10^{13}$ cm^{-2} showing a degenerate doping. Other parameters related to the performance of the WSe_2 based device like field effect mobility, threshold voltage "V_{th}" shift toward positive voltage, the ON/OFF ratio, the conductivity of the device shows an exceptional increase at this concentration level. In short p-type WSe_2 FET achieved by this way will contribute a lot in the area of optoelectronics, LEDs in the near future based on TMDs material.

References:

[1] “Controllable Nondegenerate p-Type Doping of Tungsten Diselenide by Octadecyltrichlorosilane” Dong-Ho Kang, Jaewoo Shim, Sung Kyu Jang, Jeaho Jeon, Min Hwan Jeon, Geun Young Yeom,Woo-Shik Jung, Yun Hee Jang,) Sungjoo Lee,and Jin-Hong Park, ACS Nano 1099–1107’ 2015.

[2] “Emerging Device Applications for Semiconducting Two-Dimensional Transition Metal Dichalcogenides” Deep Jariwala, Vinod K. Sangwan, Lincoln J. Lauhon, Tobin J. Marks, and Mark C. Hersam. ACS Nano,1102–1120’ 2014.

[3] “High-Performance Field-Effect-Transistors on Monolayer WSe2” W. Liu, W. Cao, J. Kang, and K. Banerjee. ECS Transactions, 281-285’ 2013.

[4] “High-Gain Inverters Based on WSe_2 Complementary Field-Effect Transistors” Mahmut Tosun, Steven Chuang,Hui Fang,Angada B. Sachid,Mark Hettick, Yongjing Lin, Yuping Zeng, and Ali Javey, *ACS Nano*, 4948–4953’ 2014.

[5] “Roll of Metal Contact in Designing High Performance Monolayer n-type WSe2 Field Effect Transistors” Wei Liu, Jiahao Kang, Deblina Sarkar, Yasin Khatami, Debdeep Jena,and Kaustav Banerjee. Nano Lett. 13, 1983−1990’ 2013.

[6] “Enhancement of Photovoltaic Response in Multilayer MoS_2 Induced by Plasma Doping” Sungjin Wi, Hyunsoo Kim, Mikai Chen, Hongsuk Nam, L. Jay Guo, Edgar Meyhofer, and Xiaogan Liang, ACS Nano,5270–5281’ 2014.

[7] “Air-Stable Surface Charge Transfer Doping of MoS_2 by Benzyl Viologen” Daisuke Kiriya, Mahmut Tosun,Peida Zhao, Jeong Seuk Kang, and Ali Javey,J. ACS, 7853−7856, 2014.

[8] “Air Stable p-Doping of WSe2 by Covalent Functionalization” Peida Zhao,Daisuke Kiriya,Angelica Azcatl, Chenxi Zhang,Mahmut Tosun, Yi-Sheng Liu,)Mark Hettick, Jeong Seuk Kang,Stephen McDonnell,Santosh KC, Jinghua Guo,) Kyeongjae Cho,Robert M. Wallace, and Ali Javey, ACS Nano 10808–10814, 2014.

[9] “Degenerate n-Doping of Few-Layer Transition Metal Dichalcogenides by Potassium” Hui Fang,Mahmut Tosun,Gyungseon Seol,Ting Chia ChangKuniharu Takei,Jing Guo,and Ali Javey, Nano Lett, 13, 1991−1995,2013.

[10] “High-Performance Single Layered WSe2 p-FETs with Chemically Doped Contacts” Hui Fang,Steven Chuang,Ting Chia Chang, Kuniharu Takei,Toshitake Takahashi,and Ali Javey, Nano Lett, 12, 3788−3792,2012.

[11] “Hole mobility enhancement and p -doping in monolayer WSe2 by gold decoration” Chang-Hsiao Chen, Chun-Lan Wu, Jiang Pu, Ming-Hui Chiu,Pushpendra Kumar, Taishi Takenobu and Lain-Jong Li. 2D Mater, 034001, 2014.

[12] Atomistix Tool Kit v. 12.2.2, Quantum Wise A/S.

[13] “Photodetectors based on graphene, other two-dimensional materials and hybrid systems” F. H. L. Koppens, T. Mueller, Ph. Avouris, A. C. Ferrari, M. S. Vitiello and M. Polini. NNANO, 10.1038, 215, 2014.

[14] “Few-Layer MoS2: A Promising Layered Semiconductor” Rudren Ganatra and Qing Zhang ACS Nano VOL. XXX ’ NO. XX ’ 000–000 ’ XXXX.

[15] “Preparation and Applications of Mechanically Exfoliated Single-Layer and Multilayer MoS2 and WSe2 Nanosheets”. Hai Li, Jumiati Wu, Zongyou Yin, and Hua Zhang. ACR, 47, 1067−1075, 2014.

[16] “Chemically Exfoliated MoS2 as Near-Infrared Photothermal Agents” Stanley S. Chou, Bryan Kaehr, Jaemyung Kim, Brian M. Foley, Mrinmoy De,Patrick E. Hopkins, Jiaxing Huang, C. Jeffrey Brinker, and Vinayak P. Dravid. Angew. Chem. Int. Ed, 52, 4160 –4164, 2013.

[17] “Electrochemical Characterization of Liquid Phase Exfoliated Two-Dimensional Layers of Molybdenum Disulfide”Andrew Winchester, Sujoy Ghosh, Simin Feng, Ana Laura Elias, Tom Mallouk,Mauricio Terrones, and Saikat Talapatra, ACS, 6, 2125−2130 2014.

[18] “Oxidation of π-conjugated polymer with gold trichloride: enhanced stability of the electronically conducting state and electroless deposition of Au^0” Muhamed S.A Abdou and steven Holdcroft. Synthetic Metals,60, 93-96, 1993.

[19] “Role of Anions in the AuCl3-Doping of Carbon Nanotubes” Soo Min Kim,Ki Kang Kim,Young Woo Jo,Min Ho Park, Seung Jin Chae, Dinh Loc Duong,Cheol Woong Yang,Jing Kong, and Young Hee Lee. ACSNano VOL. 5 NO. 2 1236–1242’ 2011.

[20] “Enhancing the conductivity of transparent graphene films via doping” Ki Kang Kim, Alfonso Reina, Yumeng Shi, Hyesung Park,Lain-Jong Li, Young Hee Lee, and Jing Kong. Nanotechnology, 21, 285205, 2010.

[21] “Metal semiconductor barrier modulation for high photoresponse in transition metal dichalcogenide field effect transistors.” Hua Min Li, Dae Young Lee, Min Sup Choi, Deshun Qu, Xiaochi Liu, Chang Ho Ra and Won Jong Yoo, Sci. Rep., 2014, 4, 4041.
[22] “Carrier transport at metal MoS2 interface” Faisal Ahmed, Min Sup Choi, Xiaochi Liu and Won Jong Yoo. Nanoscale, 7, 9222–9228,2015.

[23] http://www.cmi.epfl.ch.

[24] Single-layer Molybdenum disulfide photodetectors :MSc Thesis Oriol López Sánchez Prof. Andras Kis.

[25] “Two-Dimensional Material Nanophotonics”
Fengnian Xia, Han Wang, Di Xiao, Madan Dubey, and Ashwin Ramasubramaniam.

[26] Electron and Hole Mobilities in Single-Layer WSe2. Adrien Allain and Andras Kis. ACS VOL. 8 ’NO. 7 ’7180–7185 ’2014.
[27] Electroluminescence and Photocurrent Generation from Atomically Sharp WSe2/MoS2 Heterojunction p−n Diodes. Rui Cheng, Dehui Li, Hailong Zhou, Chen Wang, Anxiang Yin, Shan Jiang, Yuan Liu, Yu Chen,Yu Huang, and Xiangfeng Duan. ACSNano Lett, 14, 5590−5597, 2014.
[28] Vertical Heterostructure of Two-Dimensional MoS2 and WSe2 withVertically Aligned Layers. Jung Ho Yu, Hye Ryoung Lee, Seung Sae Hong,Desheng Kong, Hyun-Wook Lee, Haotian Wang, Feng Xiong,Shuang Wang, and Yi Cui. ACS Nano Lett. XXXX, XXX, XXX−XXX.
[29] Lateral heterojunctions within monolayer MoSe**2**–WSe**2** semiconductors, Chunming Huang, SanfengWu, Ana M. Sanchez, Jonathan J. P. Peters, Richard Beanland,Jason S. Ross, Pasqual Rivera,Wang Yao, David H. Cobden and Xiaodong Xu, NATURE MATERIALS,VOL 13, 2014.
[30] Near-ideal electrical properties of InAs/WSe2 van der Waals heterojunction diodes, Steven Chuang, Rehan Kapadia, Hui Fang, Ting Chia Chang, Wen-Chun Yen, Yu-Lun Chueh, and Ali Javey, APL 102, 242101, 2013.
[31] Large Area Growth and Electrical Properties of p-Type WSe2 Atomic Layers, Hailong Zhou, Chen Wang, Jonathan C. Shaw, Rui Cheng, Yu Chen, Xiaoqing Huang, Yuan Liu, Nathan O.Weiss, Zhaoyang Lin, Yu Huang, and Xiangfeng Duan, Nano Lett, 15, 709−713, 2015.

[32] Chemically Doped Random Network Carbon Nanotube p_n Junction Diode for Rectifier, Chandan Biswas,Si Young Lee, Thuc Hue Ly,Arunabha Ghosh, Quoc Nguyen Dang,and Young Hee Lee, ACS VOL. 5 ’ NO. 12 ’ 9817–9823 ’ 2011.

[33] https://en.wikipedia.org/wiki/Optical_microscope.

[35] https://en.wikipedia.org/wiki/Electron_beam_physical_vapor_deposition.

[34] http://eng.thesaurus.rusnano.com/wiki/article1093.

[36] https://en.wikipedia.org/wiki/Rapid_thermal_processing.

[37] "Rapid Thermal Processing (RTP)" Dr. Lynn Fuller, 2010.

[38] https://en.wikipedia.org/wiki/Atomic-force_microscopy.